HEATS OF IMMERSION OF ZEOLITES IN n-ALCOHOLS

by

MANUEL A. HERVAS

Thesis submitted to the Faculty of the

Virginia Polytechnic Institute and State University

in partial fulfillment of the requirements for the degree of

Master of Science

in

CHEMISTRY

APPROVED:

James P. Wightman, Chairman

John G. Dillard

Brian E. Hanson

JULY 1987

Blacksburg, Virginia

HEATS OF IMMERSION OF ZEOLITES IN n-ALCOHOLS

by

MANUEL A. HERVAS

James P. Wightman, Chairman

CHEMISTRY

(ABSTRACT)

The heats of immersion in n-alcohols of zeolites NaY, 5A and ZSM-5 and the kinetics of the immersion process have been determined using a Calvet MS-70 microcalorimeter. The specific heat of immersion decreased non-linearly as a function of chain length of alcohol for NaY and 5A. In contrast, the specific heat of immersion passed through a maximum at n-pentanol for ZSM-5. The specific immersion time as a function of chain length of alcohol showed an apparent linear increase in the order 5A > ZSM-5 > NaY. NaY showed almost no increase. The effects of sample evacuation temperature and butyl alcohol isomer bulk on the heats of immersion were also investigated. These results were interpreted in terms of molecular accessibility of the wetting liquid into the pores of the zeolites and in terms of the Si/Al ratio of the zeolites. The overall kinetics of immersion appears to be first order.

Acknowledgements

I would like to express my gratitude to my advisor, Professor James P. Wightman, for his valuable support and understanding during this work.

My appreciation to Dr. B. E. Hanson, who is a member of my committee, for providing me with some samples of zeolites and for his readiness to help in every instance.

My appreciation to Dr. J. G. Dillard, who is a member of my committee, for his valuable help and for showing a great deal of interest in my work.

I would like to thank to Dr. M. E. Davis who provided the zeolite ZSM-5 synthesized in his laboratory in the Chemical Engineering Department and for his useful suggestions.

I would like to express my appreciation to all the graduate student members of our research group of surface chemistry for their continuous help and support. Special thanks to

for his help with the microcalorimeter.

Special appreciation is given to the Ecuadorian Fulbright Commission and its counterpart in the United States for the scholarship they granted to me for pursuing graduate studies in this university.

Special thanks to the "Instituto de Ciencias Basicas" of the "Escuela Politecnica Nacional" for its auspice.

I want to thank all the people who in any way contributed to make this work possible.

Table of Contents

List of Tables

List of Illustrations

Chapter I

INTRODUCTION

Zeolite minerals have been known since the 18th century when Cronstedt (1) in 1756 recognized them as a new kind of mineral. However, zeolites remained just a curiosity for scientists until the early 20th century when zeolites attracted the attention of many researchers because of their unique physicochemical properties making them suitable for industrial applications. Probably the first practical use of zeolites was as ion exchangers for softening in water treatment plants that led to the development of synthetic, amorphous aluminosilicate commercial materials with cation exchange properties (2). Although, the cation exchange properties of zeolites were recognized as early as 1850 by Way (3). The discovery of synthetic zeolites in the early 1950's resulted in gigantic progress in zeolite technology which attracted the interest of many researchers even further due to the more uniform composition of synthetic zeolites. Since then thousands of industrial applications have been found for these materials. The recognition of the catalytic properties of zeolites and the development of new synthetic zeolites with interesting properties such as the high silica content molecular sieves and new potential processes involving these materials increased even more the spectrum of applications of synthetic zeolites. One of the most relevant potential applications of zeolites is the conversion of methanol into a high quality gasoline which is of enormous economic

importance since methanol can now be obtained from coal which is an important reserve of the United States estimated at 30% of the total world's coal reserves. The number of publications and patents is an indication of the enormous interest in these materials in the recent years. There is a rough estimate of 10,000 issued patents and 25,000 technical papers available up to 1980 (4). The study and complete understanding of the physicochemistry of zeolites is very important in order to make even more efficient use of these materials.

There is continuing interest in understanding the mechanism of liquid penetration into solids. Most of the research has centered on coal (5-9) which has a complex porosity. Zeolites by contrast have a well defined porosity. The purpose of the present work is to understand some aspects of the interactions between zeolites and n-alcohols by means of microcalorimetry and to study the kinetics of the immersion process.

Chapter II

LITERATURE REVIEW

2.1 GENERAL INFORMATION ON ZEOLITES

2.1.1 What a zeolite is

The word zeolite was introduced for the first time by the Swedish scientist Cronstedt in 1756 to designate a new type of mineral that expelled water when heated and thus seemed to boil. This word comes from the greek zein = to boil and lithos = stone (1). Molecular sieve is another term generally used for zeolites although it must be stressed that the two terms are not synonyms.

A zeolite, occurring in nature or as synthesized, is a crystalline aluminosilicate, generally containing groups I and II elements, usually K, Na, and Ca, and less frequently Li, Mg, Sr, and Ba. Higher polyvalent cation-containing zeolites can be prepared by cation exchange, such as rare earth containing zeolites (1,10).

Structurally, a zeolite is a skeleton formed by a three-dimensional network of AlO_4 and SiO_4 tetrahedra, which are called the primary building units, linked together by sharing nearly all of the oxygen atoms. The skeleton or framework consists of repeating substructure units, which are called secondary building units (SBU), giving the zeolite a well defined structure containing interconected voids or channels of defined dimensions typically 0.3 to 0.8 nm in diameter. It is these molecular dimensions which make zeolites unique and of great interest in science and technology. The voids of the zeolites are filled with water and cations which are balancing a deficiency of positive charge of the framework created by the isomorphous substitution of Si atoms by Al atoms. If the framework consisted only of SiO_4 tetrahedra, zeolites would have a neutral structure with a formula Si_nO_{2n} ; but since zeolites have Al also, the formula is $(Al_mSi_{n-m}O_{2n})^{m-}$ the m- charge being balanced by the extra-framework cations associated with the zeolites. Commonly zeolites are represented by the empirical oxide formula:

$$M_{2/n} \bullet Al_2O_3 \bullet xSiO_2 \bullet yH_20$$

where 'n' is the charge of the M cation, 'x' is generally > 2 since AlO_4 tetrahedra are joined only to SiO_4 tetrahedra and 'y' is the amount of water associated with the zeolite.

The cations are mobile in the channels and can be exchanged. Water molecules can be removed reversibly from many zeolites. Once a zeolite has been dehydrated, it can re-adsorb water or other gases, vapors or liquids selectively, according to the size of its pores and the size of the molecules. This selectivity is the reason why zeolites have been called molecular sieves also.

There are over 35 natural zeolites and more than 150 synthetic ones (4). Although some natural zeolites occur abundantly in sediments, they have not found extensive application yet because of the variability in composition. In contrast, synthetic zeolites can be obtained having a more uniform composition making them of more practical importance. Among the 150, only 12 basic types are relevant and commercially utilized (4). Gottardi and Galli (1) co-authored a book on natural zeolites from the point of view of the mineralogy and crystallography. Breck (10) has written a comprehensive book which covers most aspects of synthetic zeolites, including commercial forms, as well as mineral zeolites.

2.1.2 Classification of zeolites

Breck (10-11) has proposed a classification of zeolites based on earlier classifications. Breck's classification is based on the structure of the zeolites and consist of 7 groups according to the secondary building units (SBU). Zeolites that have common SBU belong to the same group.

2.1.3 Synthesis of zeolites

Several reviews about zeolite synthesis have been published (10,12-13). The main objectives of the synthesis of zeolites are: 1) to develop zeolites with potential technological applications and 2) to understand the complexity of the mechanism of zeolite nucleation and crystal growth. Zeolites are synthesized in an oxide system leading to a gel consisting of H_2O-SiO_2-Al_2O_3-alkali, normally below 200°C and at autogenous pressure. Somewhat different systems have been used also such as alkaline earths, lithium-sodium, tetra-alkylammonium bases and other organic cations. For example, tetra-propylammonium is essential in the synthesis of ZSM-5 (see section 3.1.1).

2.1.4 Characterization of zeolites

Numerous analytical techniques have been applied to the study of the structure and physicochemical properties of zeolites. Some of the most important techniques will be discussed next stressing those points of interest for the present work.

a) Infrared spectroscopy (IR)

Infrared spectroscopy has been used for over 20 years for the study of the framework structure of zeolites as well as the nature of the hydroxyl groups and the interaction between the cations and adsorbed molecules (10,14-15). IR studies revealed that the hydroxyl groups, the cations and the aluminum atoms can act as adsorption sites in zeolites (15). IR spectroscopy studies of NaX zeolite suggest that water molecules are bonded directly to the cations by the oxygen and water can be bonded to the oxygen atoms of the zeolitic structure by the hydrogen atoms; zeolites having a lower aluminum content were shown to bond water molecules more weakly (16). Kiselev, et al. (17) reported that the OH group of methanol adsorbed on synthetic faujasites interacts at low coverage with the cations by means of its lone pair of electrons, while at medium and high coverages, the formation of hydrogen bonds between adsorbed alcohol molecules is predominant. Methanol OH groups can weakly bond to the oxygen atoms of the skeleton of the zeolites also. IR has also been used for the study of the cation positions in zeolites (18).

b) NMR spectroscopy

NMR spectroscopy has been used for studying the mobility of water molecules, cations and other adsorbed molecules inside the zeolites as well as other properties of zeolites such as the acidity (19-21). In the past few years, ^{29}Si and ^{27}Al solid state NMR and magic-angle spinning NMR have proved to be powerful techniques for the study of the zeolite structure as well as other catalysts. ^{27}Al is more structure sensitive than ^{29}Si (22-24).

c) X-ray photoelectron spectroscopy (XPS or ESCA)

ESCA has been used to study the surface composition and acidity of zeolites. The study of the surface of zeolites is important because it is known that in many instances the catalytic activity of zeolites is limited only to the surface or to the few first unit cells below the external surface of the crystals due to diffusion limitations (25-26). Tempere and Delafosse (25) found an aluminum deficiency (an increase in Si/Al ratio) on the surfaces of NaA, NaX, NaY and other zeolites (see section 4.4).

d) X-ray diffraction (XRD)

XRD has been traditionally one of the most important and powerful techniques for the elucidation of crystalline structures (27). Breck (11) states "without x-ray diffraction, the structure of synthetic zeolites would be hopelessly confused." Because of the lack of x-ray diffraction data, many of the earlier reports about synthetic zeolites are meaningless. Jarman (28) presents a review on the application of the powder X-ray diffraction technique to the determination of the framework composition of zeolites and discusses a method for determining Si/Al ratios.

e) Electron microscopy

Electron microscopy is a universal technique widely used for studying and characterizing solids so it has been used for studying the topography of zeolite crystals (29). Some applications of transmision electron microscopy (TEM) as well as a discussion of instrumentation and methodology for the interpretation of micrographs in terms of particle size distribution are given by Aznarez, et al. (30). High resolution electron microscopy (HREM) is a powerful technique based on the ability to reveal structures with nearly atomic resolution. In contrast to most of the techniques discussed so far which give an average spatial information of the structure, HREM can reveal tiny structural imperfections in submicron size crystals (31).

f) Thermal analysis

Zeolites have the ability to lose water at high temperatures, generally in the range of 150 - 400°C, and readsorb it at room temperature from the environment. Thus thermal analysis is an important method for studying this particular property of zeolites. Four types of techniques have been used for the thermal analysis of zeolites namely, differential thermal analysis (DTA), thermogravimetric analysis (TGA), differential thermogravimetric analysis (DTGA) and differential scanning calorimetry (DSC). Gottardi and Galli (1) are of the opinion that TGA and DTGA of zeolites are more reliable and reproducible and less subject to instrumental conditions than DTA. There is not sufficient data on zeolites using DSC to make any comparison. By means of thermogravimetric studies of faujasites with different Si/Al ratios and different cationic forms, Li

and Rees (32) found that the number of water molecules per unit cell decreased linearly with increasing Si/Al ratio of those zeolites. This trend tends to support the suggestion that on increasing the Si/Al ratio, the selectivity of faujasites and other zeolites for polar molecules is decreased while the affinity for organic hydrophobic molecules is enhanced.

g) UV spectroscopy

Apparently UV spectroscopy has been used to a lesser extent than some of the other techniques. This technique has been used to investigate the nature of the acid centers in zeolites as either Bronsted or Lewis sites by analysing the nature of the ions produced on adsorption of molecules such as benzene, pyridine and cumene involving charge transfer. The identification of acid sites is important in heterogeneous catalysis (33, 34).

h) Surface area and pore volume analysis

Surface areas of powders have been calculated traditionally from adsorption isotherms using the BET equation (35). Generally nitrogen has been used as the adsorbate, taking its cross-sectional area as 0.162 nm^2 (36). Adsorption on zeolites is a matter of pore filling and therefore the BET equation is not applicable for determining the surface area of these solids, although the adsorption isotherms are of type I (10). However, authors continue to talk about surface areas of zeolites. Probably the terms "monolayer equivalent" or "equivalent surface area" are more apropriate for expressing the adsorption capacity of zeolites (10). Recently, Stakebake and Fritz (37) reported surface area measurements of different samples of chabazites and 5A zeolites. Plots of the BET equation using nitrogen adsorption data generated straight lines; however, the intercepts were negative, confirming that the BET equation cannot be applied for zeolites. The surface area for 5A was reported as 753 m^2/g obtained by the saturation method instead, which is a method of calculating surface areas based on the amount of adsorbed nitrogen at saturation indicated by the nearly zero slope of the adsorption isotherm at this point. The same authors reported other methods for measuring surface areas and porosity of zeolites such as the t-method which is based

on comparison of nitrogen adsorption on a non-porous material (taken as a reference) with adsorption on the porous sample material.

Despite the fact that crystals of synthetic zeolites are generally small, 1 - 5 μm typically, the external surface area is negligible (< 0.5%) compared with the equivalent internal surface area which is typically in the order of 800 m^2/g after dehydration. For spherical zeolite particles of 1μm in diameter, an external surface area of 3 m^2/g is calculated. Suzuki, et al.(38) described recently a method for determining the external surface area of zeolites based on nitrogen adsorption at 77 K and the previous filling of the pores of the zeolites with water, ethane, propane, butane or 2,2-dimethylpropane by adsorption. They report an external surface area of 3.7 m^2/g and a total surface area of 886 m^2/g for a sample of NaY of 0.5 - 1 μm.

i) Pore size determination

The pore diameter of zeolites is determined from the kinetic diameter of the molecules that are or are not adsorbed on the zeolites under certain given conditions (10).

j) Calorimetry

This technique will be discussed below in a separate section.

2.1.5 Uses and properties of zeolites

A great variety of applications of zeolites have been reported based on their properties (2,4). The uses and properties of zeolites can be classified into three main groups:

1. Adsorbents and molecular sieves
2. Ion exchangers
3. Catalysts

Several reviews have been published about the adsorption and molecular sieve properties of zeolites (39 - 41). Some of the major applications are: drying of organic liquids; removal of sulfur

compounds from natural gas and liquified petroleum gas; and, removal of pollutants such as Hg, NO_x, SO_x from gases.

Sherry (42) gives a review of cation exchange properties of zeolites. As ion exchangers zeolites were used at the begining of the century for water softening. They have been used for the removal and purification of radioisotopes (cesium, strontium) with the advantage that zeolites are stable to ionizing radiation and the removal of NH_4^+ from waste water.

There are several reviews on the use of zeolites as catalysts (43 - 46). Zeolites have been proposed for hydrocarbon conversion (alkylation, cracking, isomerization), organic reaction catalysts, for the conversion of methanol into gasoline and for the dissociation of water.

2.2 ZEOLITES USED IN THIS WORK

In this work three types of zeolites have been used, namely, NaY (47), 5A (48-51), and ZSM-5 (52). Those zeolites are among the most widely used in research and industry. The synthetic zeolites of commercial importance are types A, F, L, Omega, W, X, Y, Zeolon mordenite and ZSM-5 mainly in their Na^+, Ca^{2+}, NH_4^+, and H^+ forms (30).

2.2.1 Zeolite NaY

NaY is a hydrophilic zeolite that belongs to group 4 according to Breck's classification, characterized by the double 6-ring (D6R) as the SBU. This zeolite consists of β-cages (sodalite cages), linked together tetrahedrally through D6R's generating a big polyhedra cage called a super-cage which has an inside diameter of about 1.3 nm and an aperture of 0.74 nm through a 12-oxygen-ring. The opening to the beta-cage is through a 6-oxygen-ring having a diameter of 0.22 nm. The unit cell of NaY is cubic and consists of 192 TO_2 tetrahedra (T is either Si or Al). The

number of Al atoms in the unit cell varies from 48 to 76 so its Si/Al ratio varies from 1.5-3.0. There are 250 water molecules associated with one unit cell when the zeolite is fully hydrated. Figure 2.1 gives the subunit structures of this zeolite as well as of the other zeolites used in this work. Figure 2.2 shows a photograph of a model of the structure of NaY zeolite and Table 2.1 gives a summary of the characteristics of this zeolite.

2.2.2 Zeolite 5A

Zeolite 5A is a hydrophilic zeolite that belongs to group 3 of Breck's classification characterized by double 4-ring members (D4R) as the SBU (see Figure 2.1). This zeolite is made up of β-cages linked together by D4R's. The center of the unit cell is a large cavity called the α-cage, which has an inner free diameter of 1.14 nm. The access to this cage is through a 8-oxygen ring forming an aperture of 0.42 nm. Zeolite 5A is a Ca, Na form of type A zeolite. The pseudo unit cell of 5A contains 24 tetrahedra, $12AlO_4$ and $12SiO_4$ and when fully hydrated, there are 27 water molecules. The true unit cell contains 8 pseudo cells. Figure 2.3 shows a photograph of a model of the structure of zeolite 5A and a summary of the characteristics of this zeolite is given in Table 2.2.

2.2.3 Zeolite ZSM-5

Zeolite ZSM-5 is a high silica molecular sieve more recently synthesized than NaY or 5A that has proved to be of enormous interest in catalysis being able to transform methanol into a high quality gasoline (53). The subunit of ZSM-5 consist of eight 5-member rings (see Figure 2.1). This type of subunit has not been reported in any other zeolite, hence it has not been classified yet. At the same time the structure of ZSM-5 (52) and the structure of a new crystalline silica called silicalite with sieve properties having the same framework topology as ZSM-5 (54) were reported.

It must be stressed that silicalite is not considered a zeolite because it does not have Al atoms in its structure.

The subunits of ZSM-5 are connected to each other by edges, generating chains which are linked to form sheets. Finally the linking of these sheets gives the three dimensional structure of ZSM-5 indicated in Figure 2.4. The skeleton of ZSM-5 shows two types of intersecting channels: one is a zig-zag type with ten-oxygen-ring circular apertures of about 0.54 nm, and the other is a linear type with ten-oxygen-ring elliptical openings of 0.52x0.58 nm. Table 2.3 gives a summary of the characteristics of ZSM-5.

2.3 CALORIMETRY

Calorimetry has been used for the direct measurement of heats of adsorption of gases on solids and heats of immersion of solids in liquids. Hemminger and Hohne (55) have a comprehensive book of fundamentals on calorimetry including a description of the calorimeters available today. A brief description of the Calvet calorimeter is given below.

2.3.1 The Calvet microcalorimeter

The Calvet microcalorimeter consists of two equal calorimeter vessels (cells) placed in an isothermal block (thermostat) that are operated by electric compensation by means of the Peltier effect for exothermic processes and of the Joule effect for endothermic processes (reversing the current). The calorimeter vessels in which the phenomenon being studied takes place, are surrounded by thermopiles, consisting of up to 1000 thermocouples, which connect the vessels with the thermostatic block. The thermopiles are operated according to the difference or twin principle which is based on symmetrically placing two systems, made as equal as possible, in a common

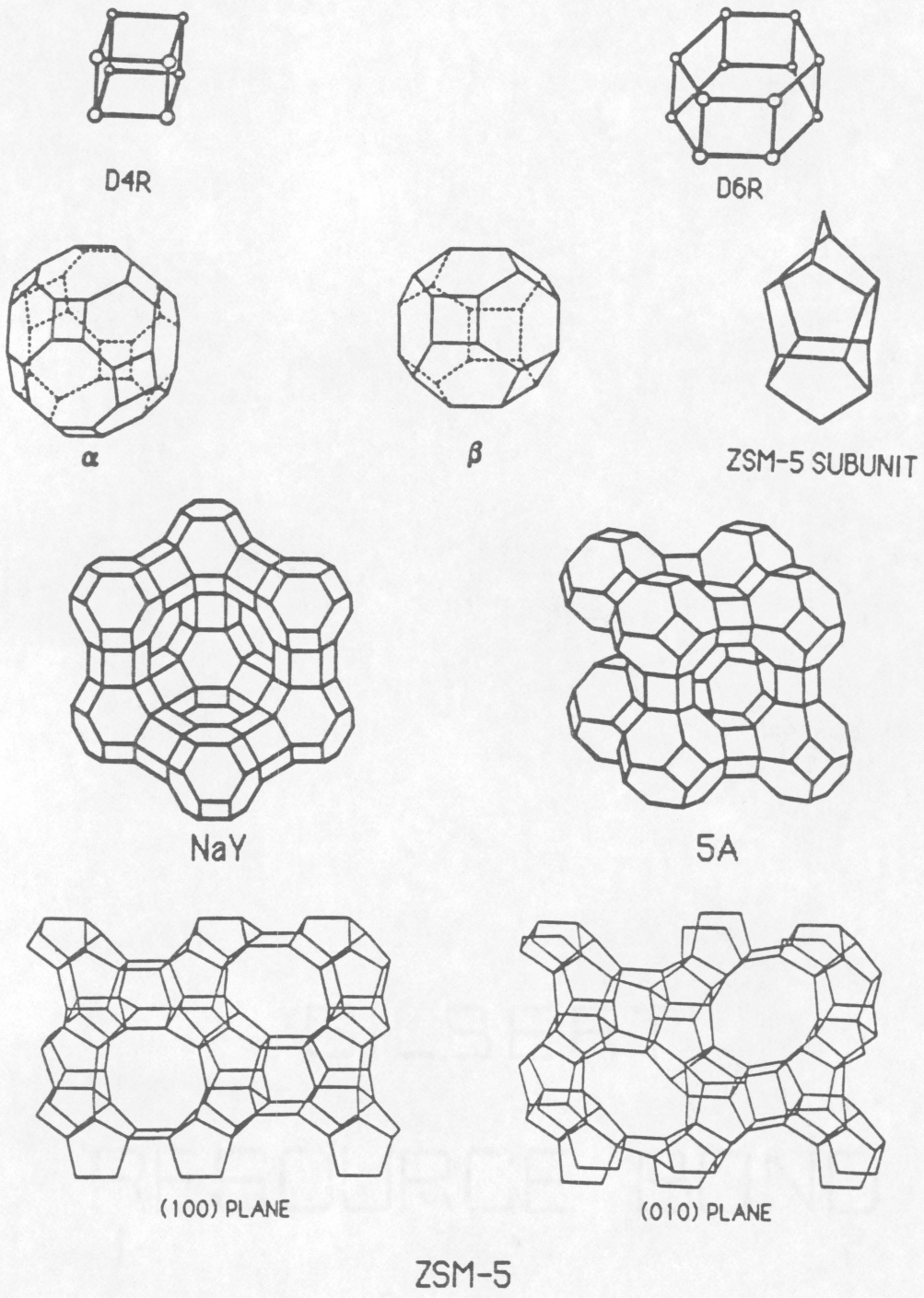

Figure 2.1. Subunits of Zeolites NaY, 5A, and ZSM-5.

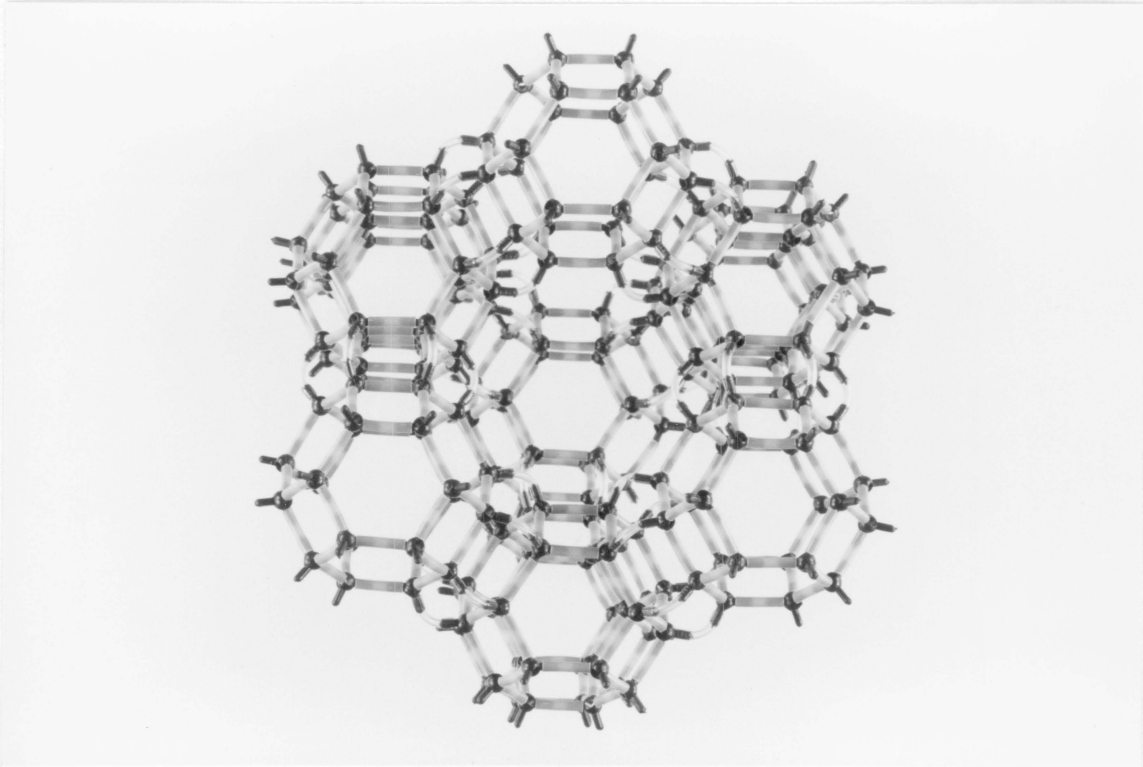

Figure 2.2. Photograph of a Model of Zeolite NaY.

TABLE 2.1

ZEOLITE NaY CHARACTERISTICS

Chemical Composition	
Typical Oxide Formula	$Na_2O \bullet Al_2O_3 \bullet 4.8\ SiO_2 \bullet 8.9\ H_2O$
Typical Unit Cell	$Na_{56}[(AlO_2)_{56}(SiO_2)_{136}] \bullet 250\ H_2O$
Variations	Na/Al 0.7 to 1.1; Si/Al = > 1.5 to ~ 3.0
Crystallographic Data	
Symmetry	Cubic
Space Group	Fd3m
Density (g/cm^3)	1.92
Unit Cell Volum (A^3)	14,901 to 15,347
Unit Cell Constant (nm)	a = 2.48 to 2.46
Structural Properties	
SBU	D6R
Framework	β-cages linked tetrahedrally through D6R Units
Void Volume (cm^3/cm^3)	0.48
Framework Density (g/cm^3)	1.25 - 1.29
Cage Type	Super Cage (26 - hedron (II)), β-Cage
Channel System	Three-dimensional, ‖ to [110]
Free Aperture (nm)	12-ring, 0.74; 6-ring, 0.22
Effect of Dehydration	Stable and reversible
Adsorption Pore Size (nm)	0.82 (Kinetic diameter of largest adsorbed molecule)

Ref. 10

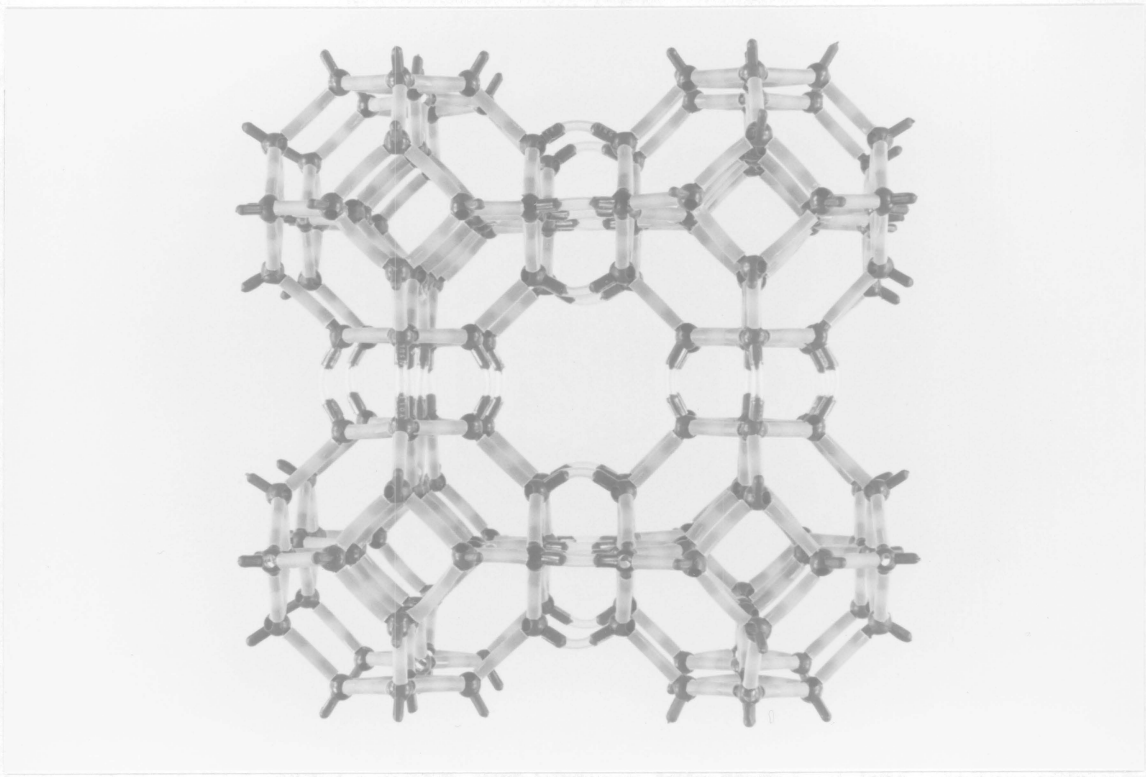

Figure 2.3. Photograph of a Model of Zeolite 5A.

TABLE 2.2

ZEOLITE TYPE A CHARACTERISTICS

Chemical Composition	
Typical Oxide Formula (5A)	$Na_2O \bullet 3\ CaO \bullet 4\ Al_2O_3 \bullet 8\ SiO_2 \bullet 18\ H_2O$
Typical Unit Cell (5A)	$Na_3Ca_{4.5}[(AlO_2)_{12}(SiO_2)_{12}] \bullet 27\ H_2O$, pseudo cell; 8X for true cell
Variations	Si/Al = ~ 0.7 to 1.2
Crystallographic Data	
Symmetry	Cubic
Space Group	Pm3m (Fm3c for true cell)
Density (g/cm^3)	1.99
Unit Cell Volume (A^3)	1870 (Pseudo cell)
Unit Cell Constants (nm)	a = 1.23 (Pseudo cell); a = 2.46 (true cell)
Strucural Properties	
SBU	D4R
Framework	Cubic array of β-cages linked by D4R units
Void Volume (cm^3/cm^3)	0.47
Framework Density (g/cm^3)	1.27
Cage Type	α, β
Channel System	Three dimensional, ‖ to [100]; 0.50 nm and ‖ to [111]; 0.22 nm
Free Aperture '5A' (nm)	0.22 into β-cage; 0.5 into α-cage
Effect of Dehydration	Stable and reversible.

Ref. 10

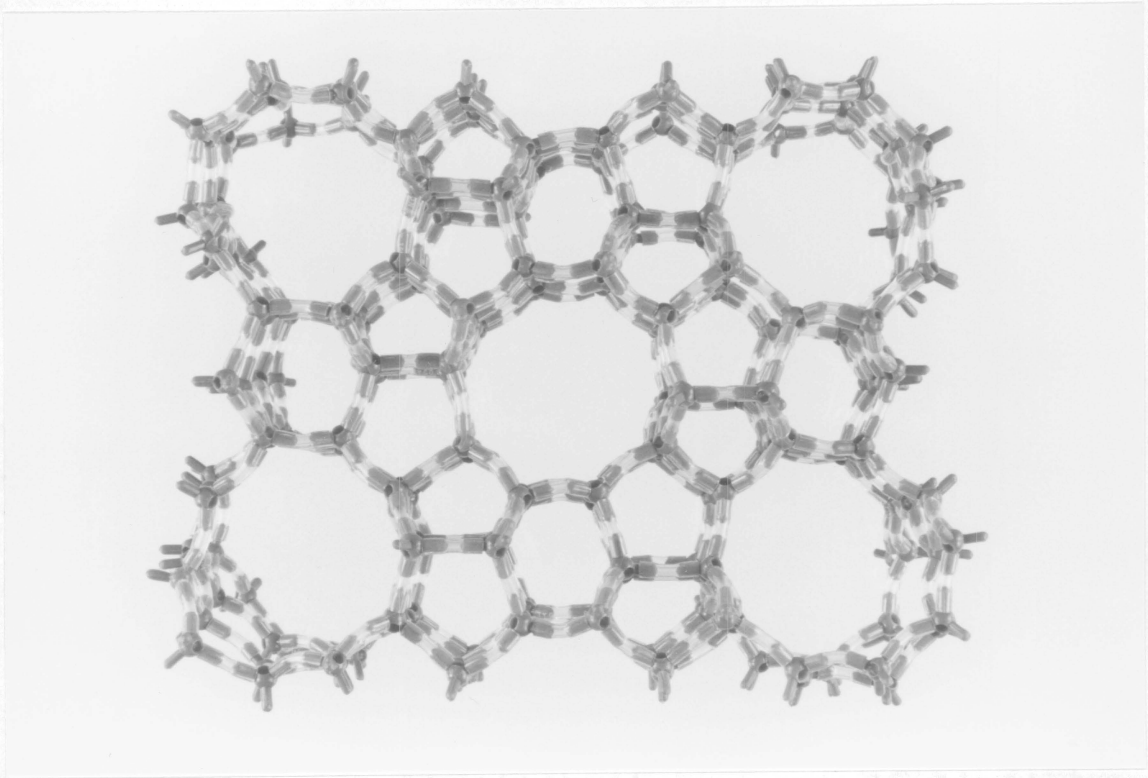

Figure 2.4. Photograph of a Model of Zeolite ZSM-5.

TABLE 2.3

ZEOLITE ZSM-5 CHARACTERISTICS

Chemical Composition	
Typical Oxyde Formula	$Na_2O \bullet Al_2O_3 \bullet 62\ SiO_2 \bullet 10.7\ H_2O$ (Na form)
Unit Cell	$Na_nAl_nSi_{96-n}O_{192} \bullet \sim 16\ H_2O$ $n < 27$ (typically $n \cong 3$)
Crystallographic Data	
Symmetry	Orthorhombic (Monoclinic has been observed also)
Space Group	Pnma
Lattice Constants (nm)	a = 2.01, b = 1.99, and c = 1.34
Channel System	Sinusoidal ∥ to [001] Straight ∥ to [010]
Void Volume (cm^3/g)	0.18; 0.10 (ref. 10)
Free aperture (nm)	10-ring Circular 0.54 ± 0.02 10-ring Elliptical 0.58 × 0.52
Adsorption Pore Size (nm)	0.6 (Kinetic diameter of largest adsorbed molecule)

Ref. 52, 54

surrounding in such a way that any disturbances such as temperature fluctuations that may occur will affect both systems equally. Since both systems are connected and a differential signal is recorded, all the disturbances are mutually offset except when a disturbance affects only one of the measuring systems such as in the case of the actual heat measurement of a reaction. Thus this type of calorimeter has a high sensitivity. The thermocouple junctions generate a thermoelectric voltage which is a measure of the temperature difference between the vessels and the surroundings. This temperature difference causes a heat flux through the thermocouples to the block.

The Calvet calorimeter is referred to as a microcalorimeter due to its high resolution of 10^{-5} W or 10^{-2} J corresponding to a temperature difference of 10^{-5} K. The disadvantage of this type of calorimeter is a large time constant of 15 - 40 minutes, which makes it unsuitable for following the kinetics of a fast reaction. Partyka, et al. (56) point out also that another disadvantage of most commercial calorimeters is the lack of continuous and effective stirring for solid suspensions, so they have adapted a device that permits agitation in the vessel of a Calvet microcalorimeter. This procedure is questionable since mechanical heat is introduced. The lack of a stirring device is rather an advantage of the Calvet microcalorimeter used in the present work since no Joule heat is introduced giving a stable base line over long periods. Hence, this type of calorimeter can detect heats evolved over long periods making it suitable for following the kinetics of slow reactions such as occurs in the immersion of solids in liquids.

2.3.2 Heats of immersion

a) Outgassing conditions

Before heats of immersion are measured, it is necessary to empty the pores of the zeolites that normally are filled with water. This is done by treating the zeolite at high temperature and low pressure for a certain period of time. Different outgassing conditions have been reported in the literature for zeolites: temperatures from 100 - 800°C, pressures from 10^{-4} - 10^{-6} torr and times from 2 - 42 hr. The more common conditions reported are a temperature of 300 - 400 °C, a

pressure of 10^{-5} torr and a time of 24 hr (37,57-61). Generally temperatures as high as 800 °C have been reported only in studies of the effect of thermal dehydration of zeolites on the structure and therefore on the heats of immersion (59,61).

b) Heats of immersion

According to Chessick and Zettlemoyer (62), heats of immersion of solids in liquids in general can provide:

1) Fundamental information about the interactions of solid surfaces with liquid molecules and the surface energy of solids.

2) The site energy distribution and other surface properties of solids. Heats of immersion as a function of coverage data are essential for this.

3) Information on the nature of adsorption from solution of two or more components.

4) Information on the hydrophilicity of solids.

5) The polarity of solid surfaces when immersed in organic liquids of different polarities.

Zettlemoyer (63) reported that the heat of immersion of polar solids is a linear function of the dipole moment of the organic liquid.

Heats of immersion results have been used to suggest that n-alcohols and n-alkanes are more ordered on the Graphon surface than n-alkanoic acids due to their quasi-solid state near the freezing point (64). Heats of immersion have been used for investigating some aspects of the chemistry and structure of coals and understanding the nature of its porosity (5-9). Surface areas of solids have been determined by heats of immersion measurements, although the direct proportionality between heats of immersion and surface area has been questioned and is a matter of disagreement (65).

Coughlan, et al. (60) studied the heats of immersion of a low sodium Y type zeolite in methanol and showed the usefulness of heats of immersion for assessing the proton acidity of this zeolite and its importance in catalysis. The heat of immersion increased almost linearly with increasing number of protons per unit cell up to replacement of 35 Na^+ cations by protons. An acceleration of the heat value was observed on replacing the remaining 20 Na^+ cations by protons.

These results were correlated with catalytic results on the competitive ethylation of toluene and benzene.

Coughlan and Carrol (66-67) reported heat of immersion data for Zeolon. The heat of immersion of Li^+, Ca^{2+} Mg^{2+}, and Sr^{2+} forms of zeolon immersed in water is governed by the energy of solvation, showing a correlation between the heat of immersion and the cation radius. Furthermore, the cations are located in the main channel sites after immersion. Barrer and Cram (58) confirm that there is an apparent relationship between the cation radius and the heat of immersion. However, this relationship is not simple because it is affected by factors such as cation screening and solvation by lattice oxygen, cation valence, number and polarizability and cation migration during hydration. A direct relationship was found between the heat of immersion per mole of lattice forming units and the magnitude of the Al/(Al + Si) ratio.

Dekany, et al. (68) reported that there is a surface energy decrease of zeolite NaY with dealumination of the zeolitic structure supported by microcalorimetric heat of immersion measurements. Messow, et al. (69) reported heats of immersion of zeolites of different hydrophilicity, including silicalite, in n-alcohols and n-alkanes. Heats of immersion of ZSM-5 and silicalite in n-alcohols are smaller than those of faujasite type zeolites due to the fact that ZSM-5 and silicalite are more hydrophobic. In section 4.5.3 results of the heats of immersion of ZSM-5 and silicalite are given and compared with those obtained in this work.

Chapter III

EXPERIMENTAL SECTION

In this chapter, a detailed description of the materials used, the experimental techniques and the procedures is given.

3.1 MATERIALS

3.1.1 Zeolites

Three types of zeolites have been used in the present work: NaY, 5A Linde and ZSM-5. All of these are commercially available and their structure and properties are well known. NaY and 5A Linde were obtained from Strem Chemical, Inc. although ultimately they came from Union Carbide Corporation which is the company that produces them. Tables 3.1 and 3.2 give a partial analysis of these zeolites (according to the manufacturer). The ZSM-5 zeolite was

synthesized in the Department of Chemical Engineering at Virginia Tech by Davis and co-workers (70). A brief description of the synthesis is given below. Table 3.3 gives a partial analysis of ZSM-5 which is the result of the average of the electron microprobe analysis of 28 particles (bulk analysis). Table 3.4 gives the unit cell formula for NaY, 5A and ZSM-5 derived from the chemical analysis.

The synthesis of ZSM-5 zeolite typically involved dissolving 0.5 g of sodium aluminate in either 0.64 or 1.83 g sodium hydroxide (50 wt %) and 10 ml distilled water. To this previous solution, 41.3 g of Ludox As - 40 colloidal silica solution (from DuPont) was added and the resulting gel was stirred to uniform consistency. Addition of the organic cation was the next step. This involved the addition of a desired quantity of tetrapropylammonium bromide (TPAB) and either tetraethylammonium bromide (TEAB) or tetramethylammonium hydroxide (TMAH) to the synthesis gel. The organic salts were purchased from Aldrich. The quantities of TPAB, TEAB, and TMAH were chosen so that the molar ratios of (TEAB + TPAB)/Al_2O_3 and (TMAH + TPAB)/Al_2O_3 were maintained at a constant value of 7.2. After the addition of the organic cation, an additional 10 ml distilled water was poured into the resulting gel. The gel compositions expressed in moles were:

A) $2.75Na_2O$-Al_2O_3-$120SiO_2$-7.2(1 - x)TPAB-7.2x(TEAB,TMAH) -$1100H_2O$

B) $6.00Na_2O$-Al_2O_3-$120SiO_2$-7.2(1 - x)TPAB-7.2x(TEAB,TMAH)-$1100H_2O$

where 'x' was varied between 0 and 1 in all cases. Once stirred to uniform consistency, the resulting synthesis gel was added to 15 ml teflon lined autoclaves and heated to 185 °C in a forced convection oven. These batches will be refered to as mixed organic cation, with batch A designated as the low sodium system and B, the high sodium system.

After some time (several hours) in which crystal growth was controlled, the teflon lined autoclaves were quenched. The solid was filtered and washed with 50 - 75 ml distilled water after which it was dried at 110°C. Afterwards the solid was placed in a crucible in a muffle furnace at a temperature of 500 - 600°C for 4 - 6 hours (calcination process) in order to burn off the organic materias that were used during the synthesis. In that way the zeolite structure was obtained free of cations other than protons and sodium.

TABLE 3.1

PARTIAL ANALYSIS OF NaY ZEOLITE

Chemical Composition (wt%-mfb)

SiO_2	63.5
Al_2O_3	23.5
Na_2O	13.0
Cl^-	< 0.05
F^-	< 0.05

Some Physical Properties

Nominal Pore Size (nm)	0.8
BET Surface Area (m^2/g)	550
Water Content (as shipped) (wt%)	23
Average Particle Size (μm)	1 - 2

TABLE 3.2

PARTIAL ANALYSIS OF 5A ZEOLITE

Chemical Composition (wt%-mfb)

SiO_2	42.93
Al_2O_3	36.49
Na_2O	5.54
CaO	15.03

Some Physical Properties

Nominal Pore Size (nm)	0.5
Hydrated Particle Density (g/cm^3)	2.03
Activated Particle Density (g/cm^3)	1.57
Particle Size (μm)	< 10
Crystal Form	Cubic
Equilibrium Water Capacity (wt%)	28

TABLE 3.3

ELEMENTAL ANALYSIS OF ZSM-5

Element	Atomic Percent	Weight Percent
Si	32.79	45.97
Al	0.44	0.59
Na	0.33	0.38
O	66.44	53.06

TABLE 3.4

UNIT CELL COMPOSITION OF THE ZEOLITES USED IN THIS WORK

Zeolite	Composition	
5A	$Ca_{4.5}Na_3[(AlO_2)_{12}(SiO_2)_{12}] \bullet 22\ H_2O$	(Pseudo Cell) (8X for True Cell)
NaY	$Na_{57}[(AlO_2)_{57}(SiO_2)_{135}] \bullet 217\ H_2O$	
ZSM-5	$Na_{0.95}H_{0.32}Al_{1.27}Si_{94.76}O_{192} \bullet 8.2\ H_2O$	

The ZSM-5 zeolite used in these experiments was obtained from the low sodium system (A). It has a Si/Al ratio of 74.

3.1.2 Polymer

One type of cross-linked polymer was used in this work. Poly-Sep AA-200 from Polysciences, Inc. Poly-Sep AA is a cross-linked polyacrylamide, whose characteristics are indicated in Table 3.5. According to the manufacturer, gel pore size has been controlled by varying the percentage of the N,N′ - methylenebisacrylamide cross linker. The polymer beads are strongly hydrophilic and do not contain ionic substituents. Poly-Sep AA swells in water, saline solutions and polar solvents such as ethylene glycol. Swelling equilibrium is established in 6 - 8 hours.

3.1.3 Reagents

The high purity (spectrophotometric grade or anhydrous) alcohols and reagents used in these experiments were from Aldrich Chemical Company, Inc. except for dodecanol which was obtained from Eastman Kodak.

All of the liquids were kept in contact with type 3A molecular sieves from Fisher Scientific Co. to avoid moisture uptake from the environment except ethanol which was anhydrous and was used immediately after opening and dodecanol which was a solid at ambient temperature.

TABLE 3.5

CHARACTERISTICS OF POLY-SEP AA 200

Exclusion Limit of Mol. Weight	200000
Range of Fractionation (mol. weight)	80000 - 200000
Water Regain (g/g)	15.0
Swelling (ml/g)	32-36
Particle Size (μm)	100-320

3.2 EXPERIMENTAL TECHNIQUES AND GENERAL PROCEDURES

3.2.1 Thermogravimetric analysis

Thermogravimetric analysis (TGA) was performed for the zeolite samples using a DuPont 1090 thermobalance. About 12 mg of sample was loaded in the platinum weighing pan of the instrument. The temperature was increased at a rate of 20°C per minute from 50 to 1100°C. The sample was run under a nitrogen atmosphere. The weight loss was recorded and plotted as a function of temperature.

The thermogravimetric analysis is of importance because it gives information about how strongly the water molecules are bound to the zeolite inside the pores; it also indicates the outgassing temperature necessary to ensure a complete removal of water from the zeolites. The resulting anhydrous structure should have a maximum pore volume to interact with the immersion liquid during the calorimetric studies.

A Perkin-Elmer TGS - 2 thermobalance was used for the polymer Poly-Sep AA 200. About 10 mg of sample was necessary. The temperature was increased at a rate of 10 °C/min from 50 to 750 °C analysis was performed under a nitrogen atmosphere.

3.2.2 Surface area analysis

A Micromeritics AccuSorb 2100E surface area analyzer was used for the surface area determinations of the zeolites. About 0.1 gram of sample was outgassed at approximately 200 °C for 24 hours at 1 x 10^{-5} torr prior to surface area measurements. Nitrogen was used as the

adsorbate for the surface area analysis. The temperature during the measurements was 77 K. The cross sectional area of the nitrogen molecule was taken as 0.162 nm^2 (36).

3.2.3 Scanning electron microscopy

Scanning electron microscopy (SEM) is a powerful technique for the analysis and characterization of solids. A Philips EM 420 T electron microscope was used to characterize the zeolite powders and the polymer. A magnification from 200X to 25000X was used. The samples were mounted on copper tape and sputtered with Pd/Au to avoid charging effects.

3.2.4 X-ray photoelectron spectroscopy

X-ray photoelectron spectroscopy (XPS) or electron spectroscopy for chemical analysis (ESCA) is an analytical technique which gives information about the surface of the material to a depth of about 5 nm. The kinetic energy (KE) of the photoelectrons, that are ejected due to the bombardment of the surface of the material with x-rays of energy hν, is measured. The binding energy (BE) is the minimum amount of energy necessary to eject an electron from an atom. This binding energy is characteristic of every element and therefore is used to identify that element on the surface of the sample. The following expression is used to correlate the measured KE and the unknown BE:

$$h\nu = BE + KE + \varphi \qquad (3.1)$$

where φ is a charging correction.

The samples were mounted on double stick sided Scotch tape and analyzed using a Perkin-Elmer PHI 5300 ESCA system. A magnesium x-ray source was used. The pressure in the spectrometer was typically 10^{-7} torr. The take-off angle was 90 degrees.

3.2.5 Outgassing process

About 50 mg of the zeolite sample was weighed to the nearest hundredth of a milligram in a glass bulb or ampoule. The ampoule was made so that it had an easy-to-break tip at the end which could be broken by a slight push. The sample bulb was attached to a vacuum line and was evacuated (outgassed) at an approximate pressure of 1 to 10 x 10^{-5} torr, typically for 24 hours at 360°C. Some other conditions were explored initially as discussed below. At these conditions it is assumed that no water is left in the intracrystalline void volume of the zeolites. A schematic diagram of the vacuum line is shown in Figure 3.1.

A custom furnace was used to maintain the outgassing temperature. The temperature was controlled by a variable autotransformer by trial and error until obtaining the desired temperature. The bulbs were inserted in the furnace which was filled with Ceramfab fiber (an asbestos substitute from Lab Safety Supply Co.) to maintain a steady temperature. The evacuation process was done very carfully to avoid loss of zeolite since the small particles could be readily sucked up into the vacuum system. To avoid this problem, a by-pass with a restriction connecting the bulbs and the vacuum line was opened first. Afterwards, the ampoules were sealed off under vacuum so that its length was about 4 cm in order to fit in the calorimeter cells.

3.2.6 Heats and kinetics of immersion

The heats and kinetics of immersion of the zeolitic and polymeric materials were determined using a Setaram Calvet MS 70 microcalorimeter at a constant temperature of 36.5°C. The sealed ampoules with sample, prepared as described above, were placed inside the calorimeter cells (stainless steel vessels) which contained 3 ml of immersion liquid. The entire assembly was previously cleaned with acetone. The distance of the ampoule tip from the bottom of the cell was carefully adjusted to about 2 mm. After the system (calorimeter + sample) reached equilibrium,

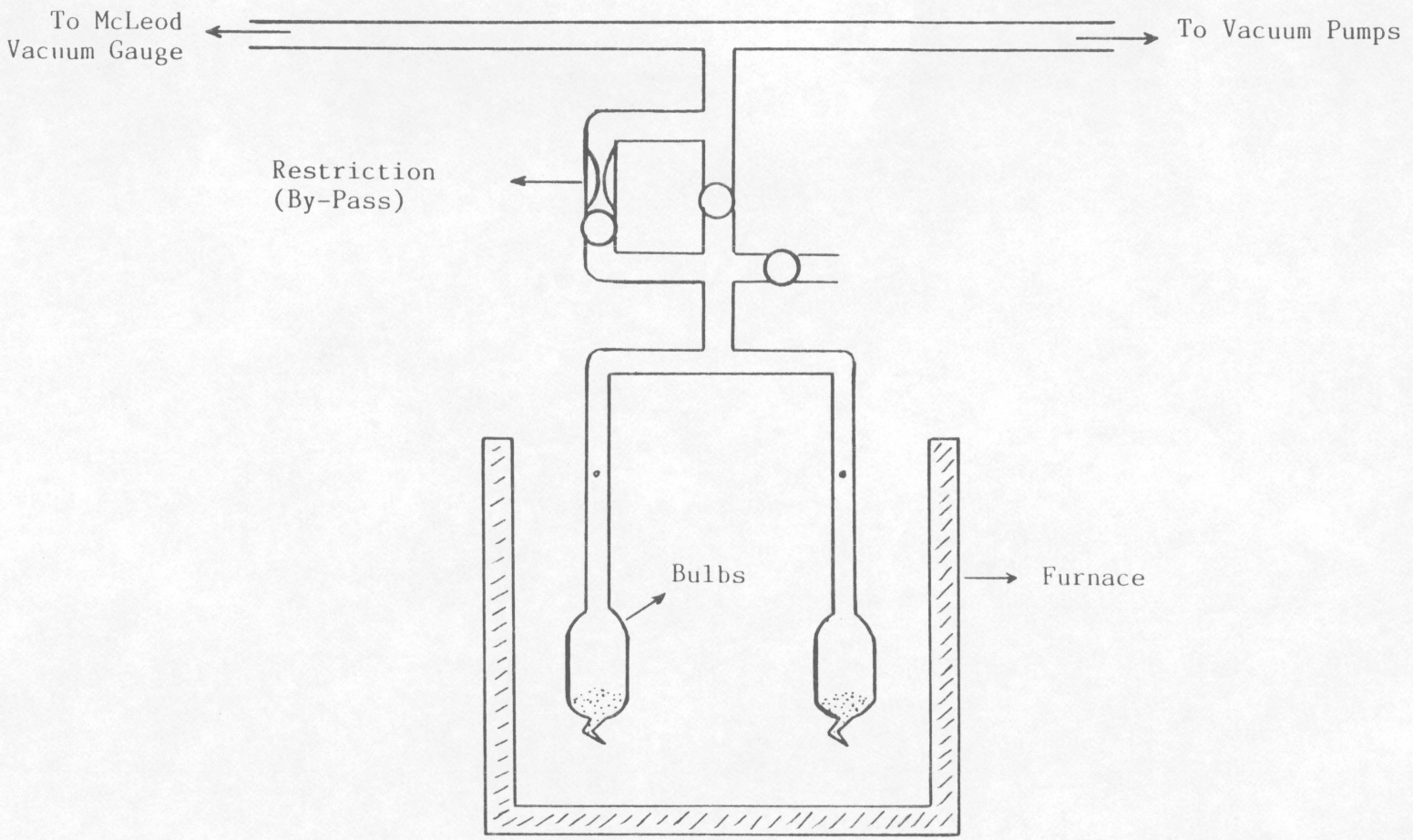

Figure 3.1. Schematic Diagram of the Vacuum Line (not to scale).

which required several hours, typically overnight, the ampoule tip was broken by pushing externally the calorimeter rod.

The heat obtained from contact of the sample and the immersion liquid is detected by a thermocouple pile in the calorimeter; some of its characteristics are given in Table 3.6. The output electrical signal generated by the pile due to the flux of heat is amplified and electronically integrated. The integral counts are recorded and printed on a paper tape at regular intervals of 100 seconds. The counts are in arbitrary units and therefore must be converted into Joules by calibration as described below. The signal is directly proportional to the heat flux and so are the counts which, after conversion to Joules, gives the "Heat of Immersion" of the sample.

The Calvet microcalorimeter has 4 chambers which holds 4 cells of 15 cm^3 of volume, 17 mm in diameter and 80 mm in height. Cells #1 and #2 are paired together and so are #3 and #4. One set is used as a reference while the other is used as a sample. The order is then reversed. A schematic diagram of a sample cell and the microcalorimeter is shown in Figure 3.2.

After the heat of immersion is released, the microcalorimenter re-attains steady state which is determined when the same count is printed for at least 5 times. The calorimeter will remain stable at this base line indefinitely if there is no further thermal perturbation. The time from breaking the tip to the final steady state can be defined as the total time necessary for complete heat release, in other words it is the "Immersion Time". The "Specific Time of Immersion" is defined as the immersion time per unit mass of sample.

There is some heat dissipation involved in the mechanical action of breaking the bulb tip such as friction, pressure - volume work when the liquid is sucked inside the bulb and the tip breakage itself. Therefore, it is necessary to measure the heat released or absorbed by an empty bulb (blank) treated in the same way as for those containing the samples; this measurement is subtracted from those of the samples.

The heat of immersion $\Delta_{im}H$ is determined by the following relationship:

$$\Delta_{im}H = \frac{S(C_t - C_r)}{W} \qquad (J/g) \qquad (3.2)$$

where C_t is the number of sample counts, C_r is the number of empty bulb counts, S is the sensitivity and W is the weight of the dehydrated sample.

TABLE 3.6

CHARACTERISTICS OF THE SMALL PILE OF THE CALVET MICROCALORIMETER

Type of Thermocouple	chromel-constantan
Number of Thermocouples	124
Nominal Sensitivity (μV/mW)	15.
Approx. Internal Resistance (Ω)	11.

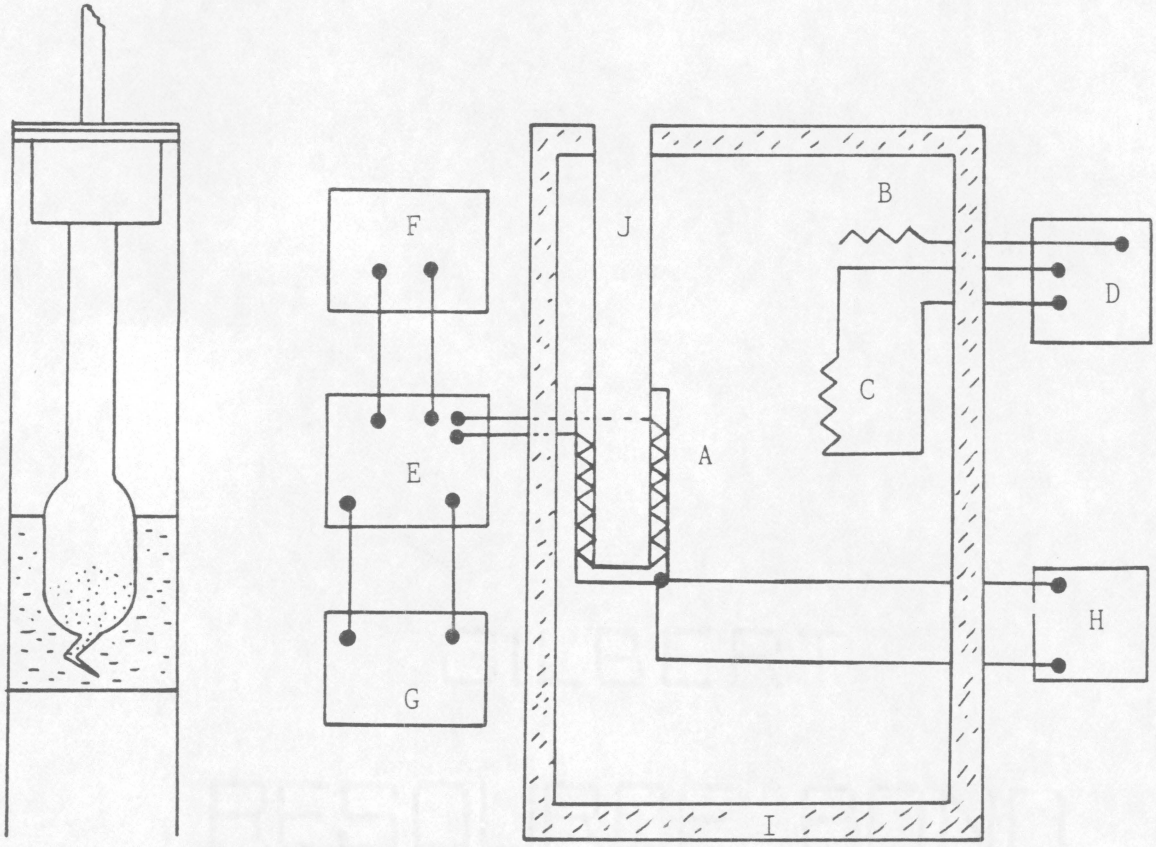

Figure 3.2. Block Diagram of Microcalorimeter and Sample Cell.

A. Microcalorimetric Detector (Thermocouple Pile)
B. Temperature Regulator Probe
C. Temperature Regulator Heater
D. Temperature Regulator
E. Amplifier
F. Recorder
G. Integrator
H. Potentiometer
I. Insulation
J. Sample Well

The cell sensitivity is determined by electrical calibration of the microcalorimeter which is performed by passing a known current (I), typically $\sqrt{30}$ mA, for a given time (t), generally 2 min., through a precision resistor in the cell whose resistance (R) is 1001.7 ohms. The sensitivity was determined by the following expression:

$$S = I^2Rt/C_t \qquad \text{(J/count)} \qquad (3.3)$$

where C_t is the total number of counts obtained during the calibration. The average sensitivity for the four cells was $2.107 \times 10^{-3} \pm 0.040 \times 10^{-3}$ The sensitivities do not change significantly within at least one year.

The settings for the amplifier during calibration and during sample runs are a 2 second response time and a sensitivity of 250μV. All runs are made at the "PS" position which sets the small thermocouple pile.

Chapter IV

RESULTS AND DISCUSSION

4.1 THERMOGRAVIMETRIC ANALYSIS

The TGA results of zeolites NaY, 5A and ZSM-5 are shown in Figure 4.1. The weight loss of zeolite NaY is the largest, 22.7 %, then 5A with a loss of 18.9%, and finally ZSM-5 with only a 2.5 % loss. It is assumed in this work that the weight loss is only due to the release of water contained in the intracrystalline structure of the zeolites and there is no contribution from any other adsorbate. Furthermore, the zeolites used have a stable structure up to relatively high temperatures, and so no reaction or degradation of the material is possible at 360 - 380 °C, the outgassing highest temperature used in the calorimetric studies, beyond the loss of intracrystalline water.

It is observed that there is about a 20% difference in intracrystalline water content for both the NaY and 5A zeolites. This small difference is expected since NaY and NaA have about the same inner void volume per unit mass of 0.34 and 0.30 cm^3/g, respectively. It is assumed that 5A

has approximately 0.30 cm^3/g since it is structurally similar to NaA but some of the Na cations have been replaced by Ca, which is a smaller ion. Both zeolites have a high affinity for water.

Due to their hydrophilic nature both NaY and 5A bind water molecules very strongly. Thus, a relatively high outgassing temperature is needed in order to remove all of the water contained in those structures as can be inferred from the TGA results. It is apparent that 5A binds water molecules more strongly than NaY since a weight loss for 5A is appreciable up to temperatures as high as 700 °C as shown in the TGA diagram. Also the specific heat of immersion 5A in water is higher than that of NaY as will be discussed later. Heats of immersion are related to the strength of the interaction between the adsorbate and the adsorbent structure. In contrast, NaY releases all of its intracrystalline water at temperatures close to 400 °C.

The water content of ZSM-5 is much smaller than that of the other two zeolites not only because of a substantially lower intracrystalline void volume of 0.10 cm^3/g (10), but because of its high Si/Al ratio, resulting in a hydrophobic structure.

The zeolites without any treatment were kept in air tight containers and showed no significant difference in their water content after three months; a maximum change of 3 % was recorded for NaY during this time. Therefore, the values for the water content in the zeolites were assumed to be constant throughout the experimentation period and were used to calculate the heats of immersion on the basis of unit weight of dehydrated zeolite.

A TGA plot for Poly-Sep AA is given in Figure 4.2. It is apparent that the initial weight loss is due to water absorbed in the polymer. Above 200°C, the polymer undergoes a thermal degradation showing a very rapid weight loss around 450°C with a residual weight of 14 %.

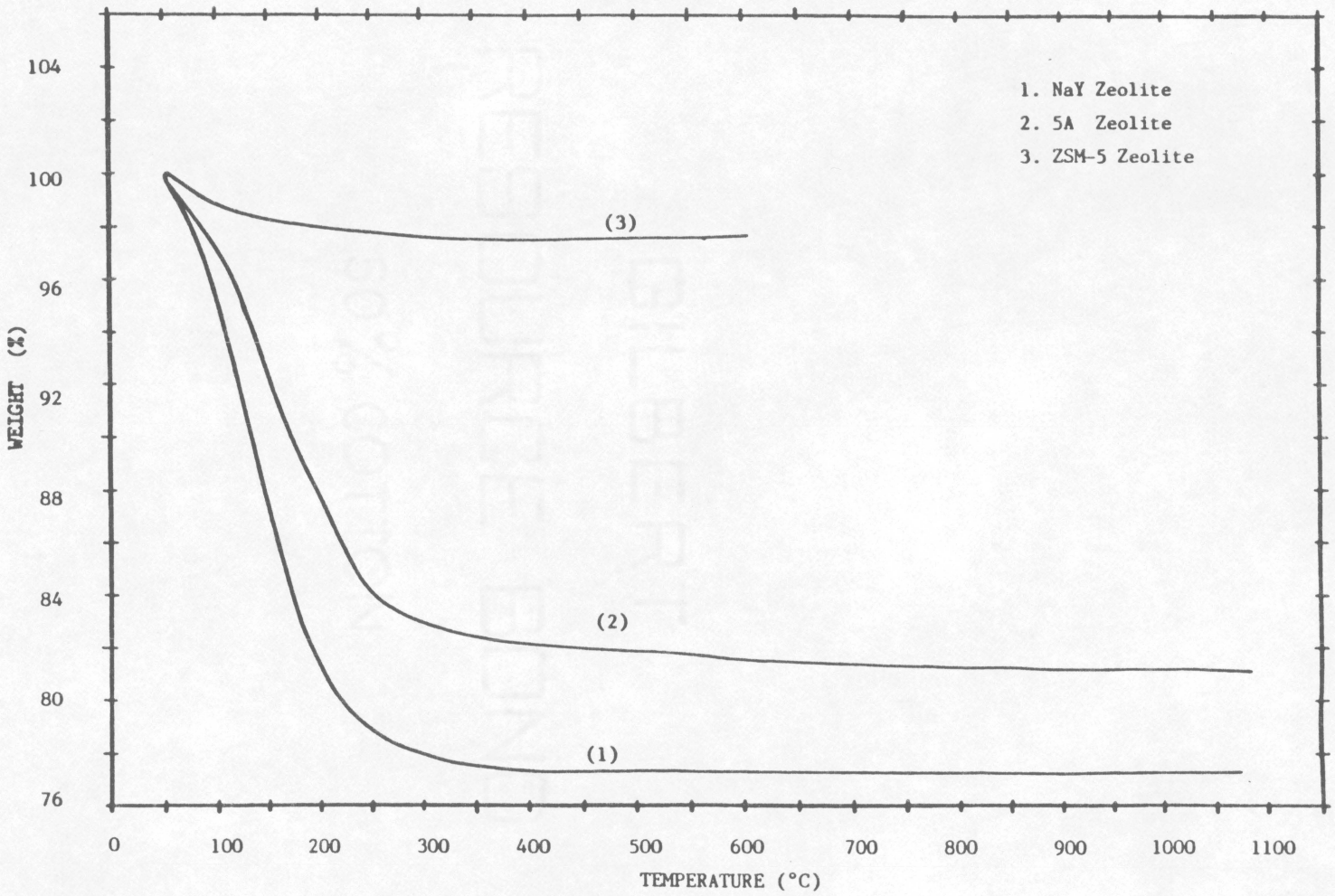

Figure 4.1. TGA Diagrams of Zeolites.

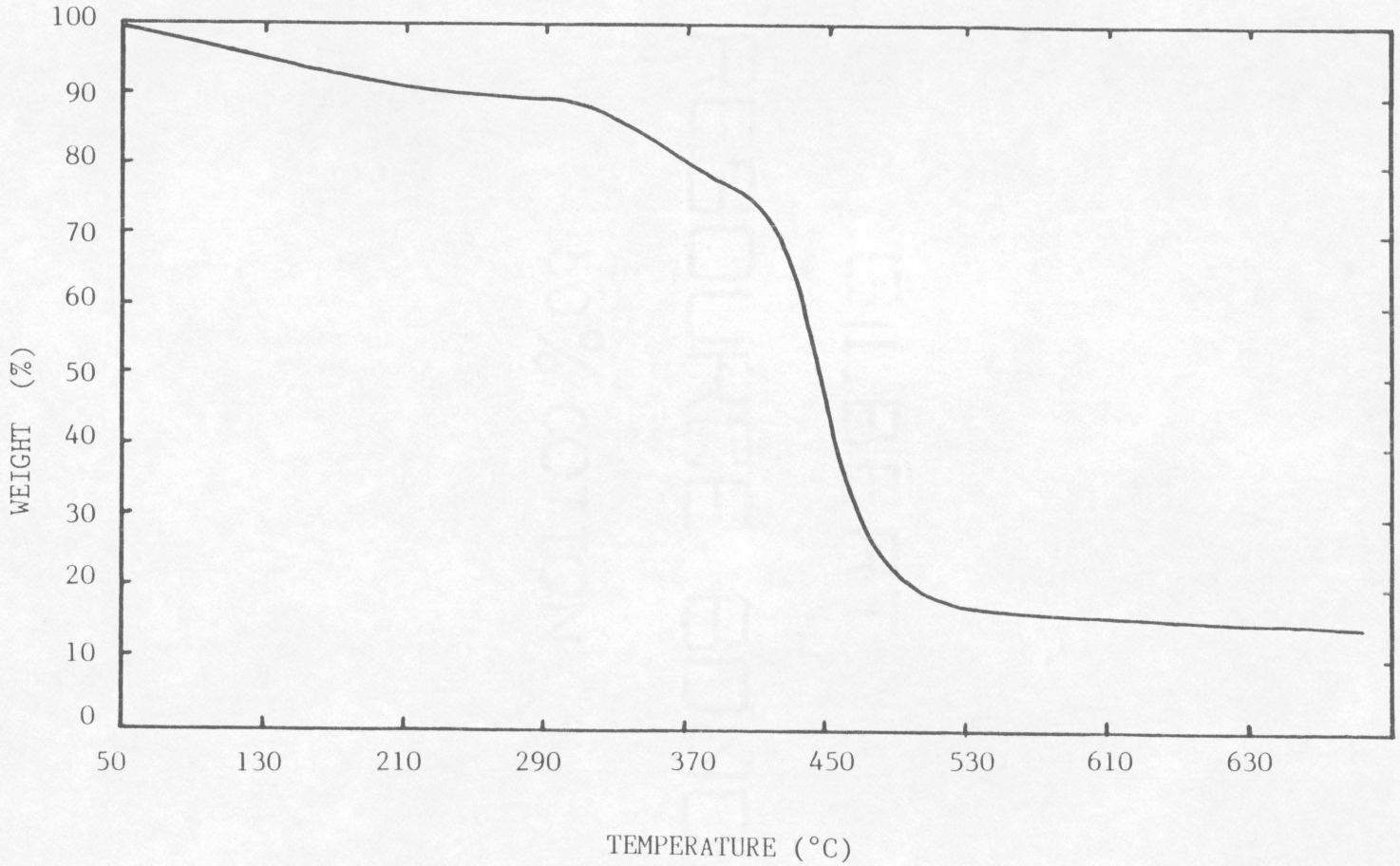

Figure 4.2. TGA Diagram of POLY-SEP AA 200 .

4.2 *SURFACE AREA DETERMINATION*

The BET surface area analysis gave values of 736 ± 74 and 531 ± 21 m^2/g for NaY and 5A respectively, expressed on the basis of anhydrous zeolite. The surface area of 550 m^2/g for NaY was given by the manufacturer (see Table 3.1).

Although zeolites typically follow type I adsorption, the BET equation is not applicable to them because adsorption in zeolites is rather a matter of pore filling. Thus, the surface area of these materials as determined by physical adsorption of nitrogen has no real physical significance in contrast to other solid adsorbents (10). Yet the measured surface area can give relative information about the adsorption capacity of the zeolites. The term "monolayer equivalent" is used sometimes in reference to the adsorption capacity of zeolites. It is assumed that the adsorbed molecules are spread out in a close-packed monolayer (10). So monolayer equivalent is probably a more appropriate term to use instead of surface area and will be adopted here.

In addition, it has been suggested that nitrogen cannot enter the β-cages of NaY or 5A at liquid nitrogen temperatures; the β-cages have an aperture of about 0.22 nm while the kinetic diameter of nitrogen is 0.364 nm. At relatively high temperatures, the vibration of the oxygen atoms localized at the aperture of the cages will permit the nitrogen molecules to get in but at 77 K nitrogen will not get in. Furthermore, it has been found that adsorption of nitrogen on zeolites generally gives larger values of pore volume due to the fact that the average density of the adsorbed phase at saturation is believed to be about 25 % greater than that of normal liquid nitrogen at 77 K. Adsorption of water on zeolites has been reported to lead to larger values of pore volume also (10).

Dubinin (71) has calculated the surface area and intrazeolitic void space for type A zeolites based on the known crystal structure. The calculated values are 1640 m^2/g and 0.278 cm^3/g, respectively. This theoretical surface area is high compared to measured values while the value of the intracrystaline volume is too low.

From the data of water content obtained from the TGA diagrams, a monolayer equivalent of 1228 and 975 m^2/g for NaY and 5A, respectively can be calculated taking the cross-sectional area for an adsorbed water molecule as 0.125 nm^2, the value recommended by McClellan and Harnsberger (36).

Finally the fact that the outgassing temperature during the surface area measurement, was relatively low of about 200°C may have contributed to the discrepancy between the absolute values of surface area and monolayer equivalent. On the other hand the ratio of the surface areas and the monolayer equivalents are similar.

4.3 SCANNING ELECTRON MICROSCOPY

Figures 4.3, 4.4, 4. 5, and 4.6 show the SEM photomicrographs of the zeolites NaY, 5A, ZSM-5 and the polymer Poly-sep AA. NaY reveals a very uniform particle size distribution of about 1 - 2 μm. Some aggregation of particles can be observed. It is known that the symmetry of the crystals of NaY is cubic. The SEM photomicrographs of NaY reveal the cubic symmetry of this zeolite although many irregularities are evident. Probably some of the particles are a result of crystal fracture.

In contrast, the SEM photomicrographs of 5A reveal perfect cubic crystals. Particles from 2 - 10 μm are displayed. Some aggregations are apparent in a multi-layer type structure. EDAX analysis of the cubes and multi-layer type
aggregates showed no significant chemical differences.

ZSM-5 shows a quite uniform particle distribution with crystals of about 20 μm and larger. The orthorhombic symmetry of these particles is revealed, although some irregularities are seen at the edges probably due to defects in crystal growth or crystal fracture since this zeolite must be brittle since it has the same structure and almost the same chemical composition as silicalite and it is known that silicalite is very brittle and its crystals can break easily during handling (72).

(a)

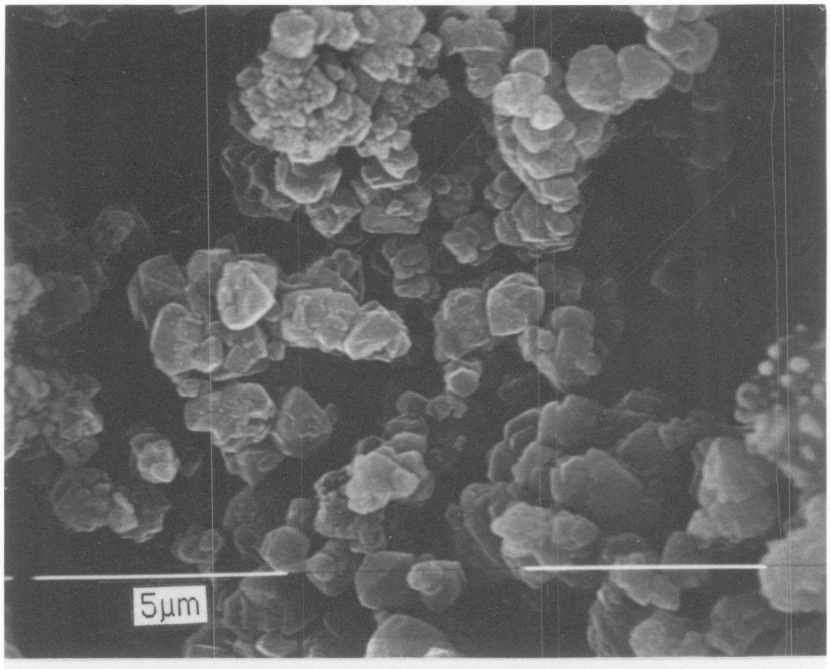

(b)

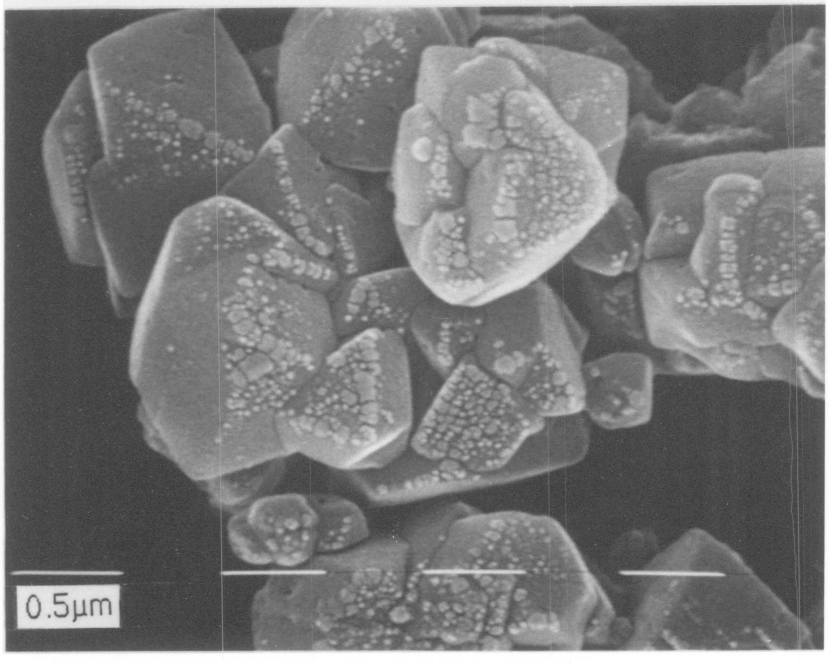

Figure 4.3. SEM Photomicrographs of NaY Zeolite.

(a) 6400X (b) 25000X

(a)

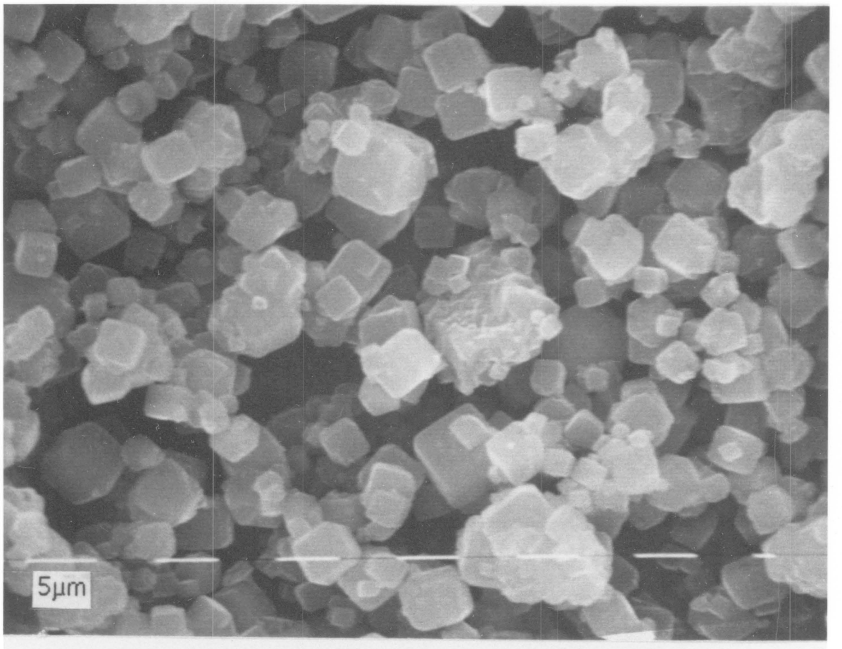

(b)

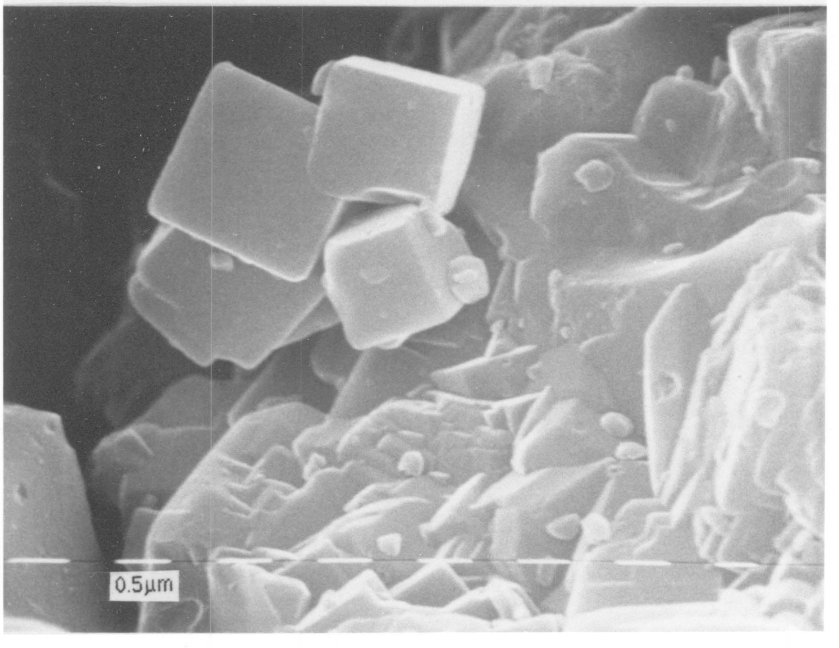

Figure 4.4. SEM Photomicrographs of 5A Zeolite.

(a) 1600X (b) 12,500X

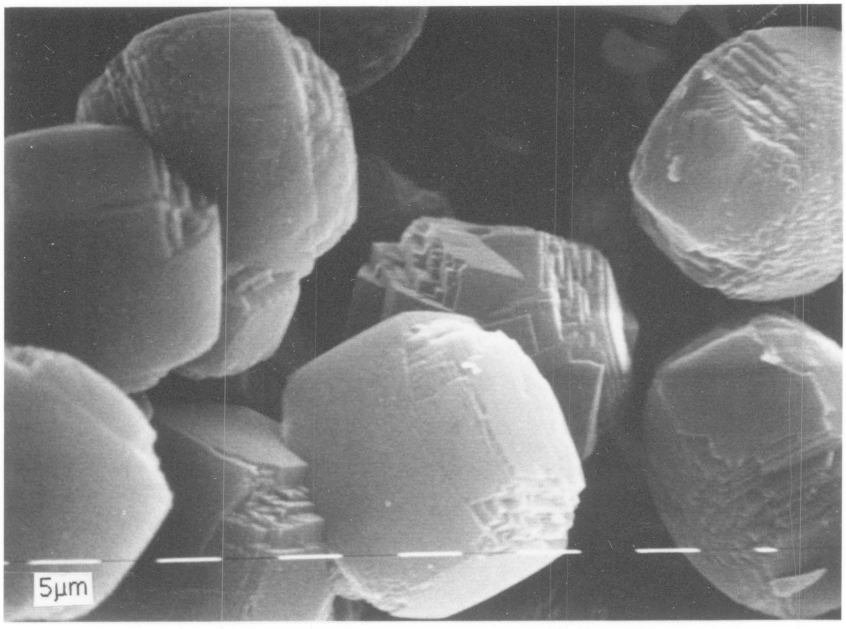

Figure 4.5. SEM Photomicrograph of ZSM-5 (1600X).

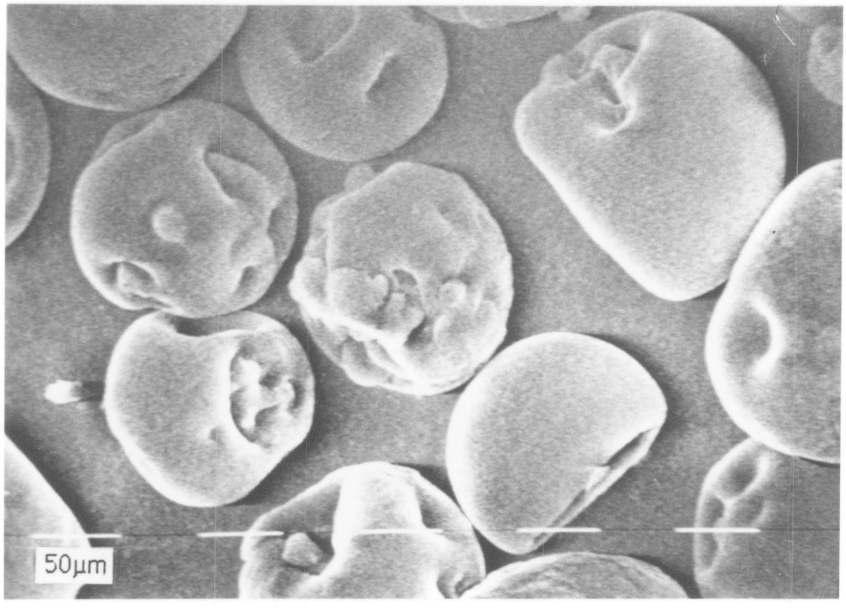

Figure 4.6. SEM Photomicrograph of Poly-Sep AA (200X).

Figure 4.6 shows dimpled round particles of Poly-Sep AA with diameters > 100 μm.

4.4 X-RAY PHOTOELECTRON SPECTROSCOPY

The wide scan ESCA spectra for zeolites NaY, 5A, ZSM-5 and Poly-Sep AA are shown in Figures 4.7, 4.8, 4.9 and 4.10, respectively. Table 4.1 gives the detailed ESCA results and Table 4.2 shows the comparison between the bulk and the surface analysis. It is first noticed that carbon, which is not a component of the zeolites, is found on the surface of all three zeolites and it is higher for 5A and ZSM-5. This surface contamination is expected from carbon-containing compounds adsorbed from the atmosphere. Therefore, the surface atomic fractions of Si, Al, Na, and Ca given in Table 4.2 are expressed as ratios to minimize the effect of ubiquitous carbon.

In zeolites, the ratio of cation charge concentration to aluminum concentration is unity since a zeolite as a whole is a neutral structures. However, it can be seen that the surface Na/Al ratio for NaY is 2.4, for ZSM-5 is 3.1, and 2XCa/Al + Na/Al is 0.7 for 5A.

With respect to Si/Al ratio, NaY (1 - 2 μm) and 5A (2 - 10 μm) show an increase of about 40% in Si/Al ratio on the surface compared to the bulk, while ZSM-5 (≅ 20 μm)shows a 4 fold decrease in Si/Al ratio on the surface in comparison with the bulk. These results can be compared to the results of Von Ballmoos and Meier (73) who have found that in 100 μm single crystals of ZSM-5, the aluminum concentration varies gradually from the center to the edges of the crystal, with the aluminum concentration up to 5 - 10 times greater near the edges than in the center. Lyman, et al. (74) found the same trend for particles of about 2 μm of Na-ZSM-5 (Si/Al = 40) but the reverse tendency for small particles of about 0.3 μm (Si/Al = 10) of the same type of zeolite. The same authors did not find a significant variation for particles of 2.2 μm of NaA (Si/Al = 1.0).

The atomic fractions of Poly-Sep AA calculated from the empirical formula of a typical polyacrylamide are about 0.64 for carbon, 0.18 for oxygen and 0.18 for nitrogen (neglecting

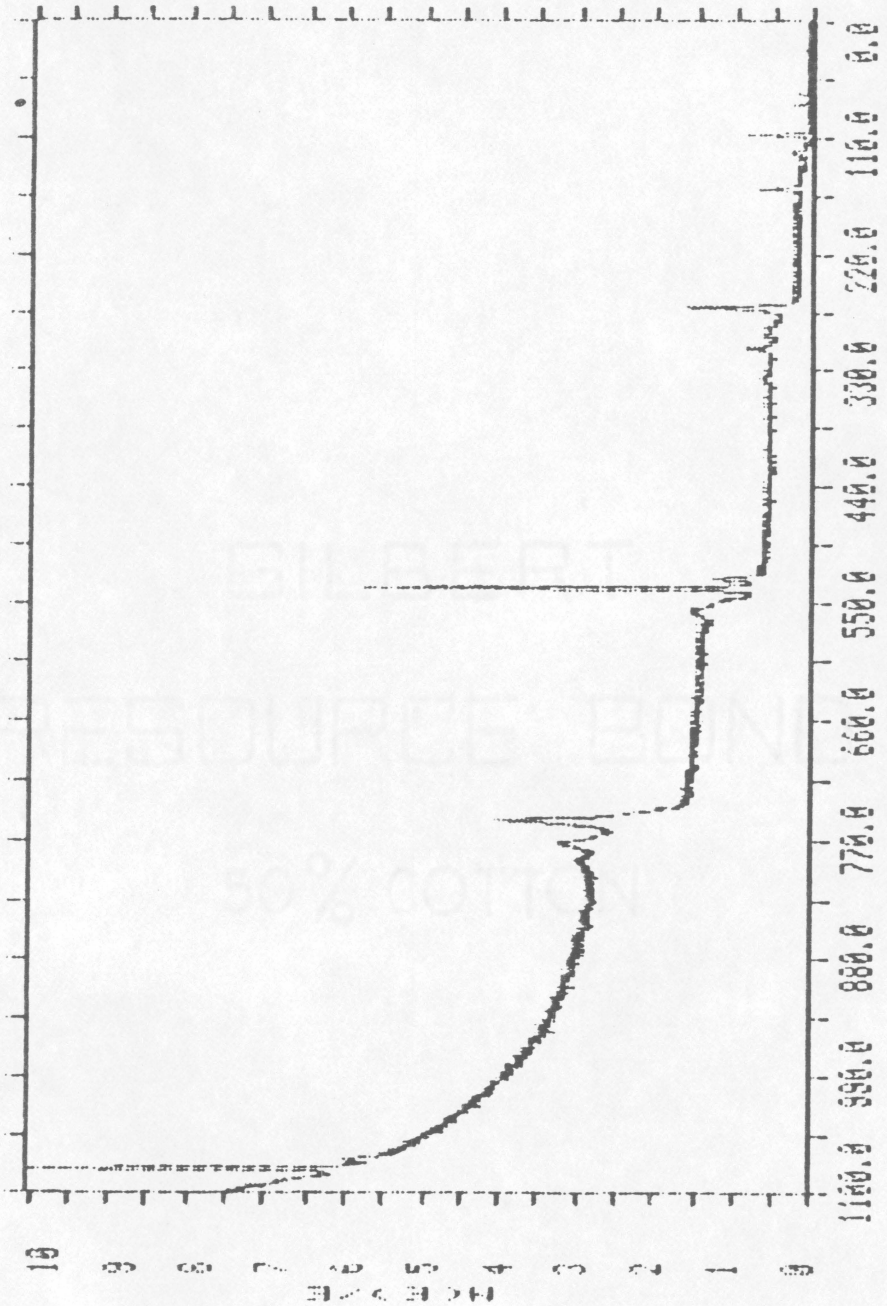

Figure 4.7. ESCA Spectrum of NaY Zeolite.

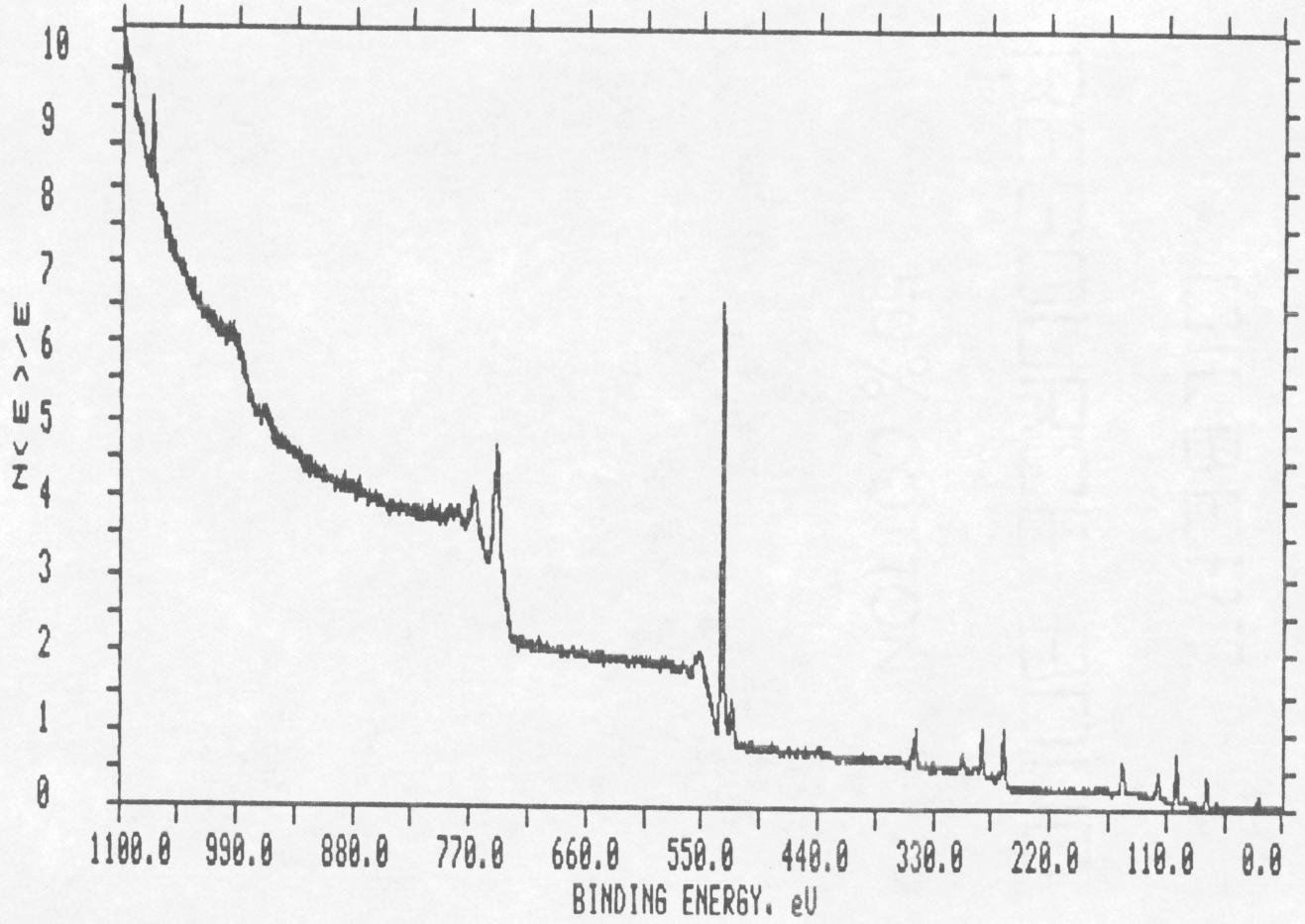

Figure 4.8. ESCA Spectrum of 5A Zeolite.

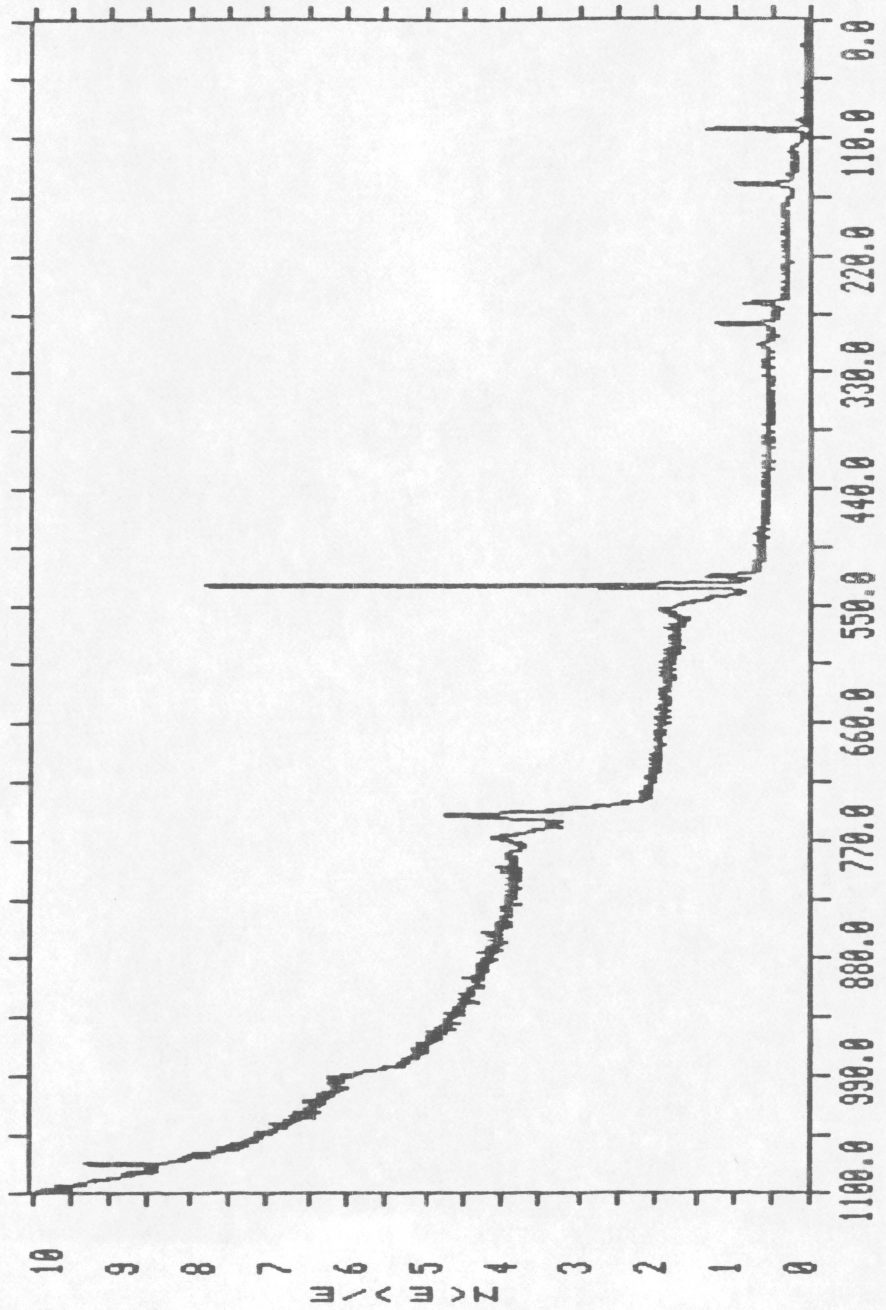

Figure 4.9. ESCA Spectrum of ZSM-5 Zeolite.

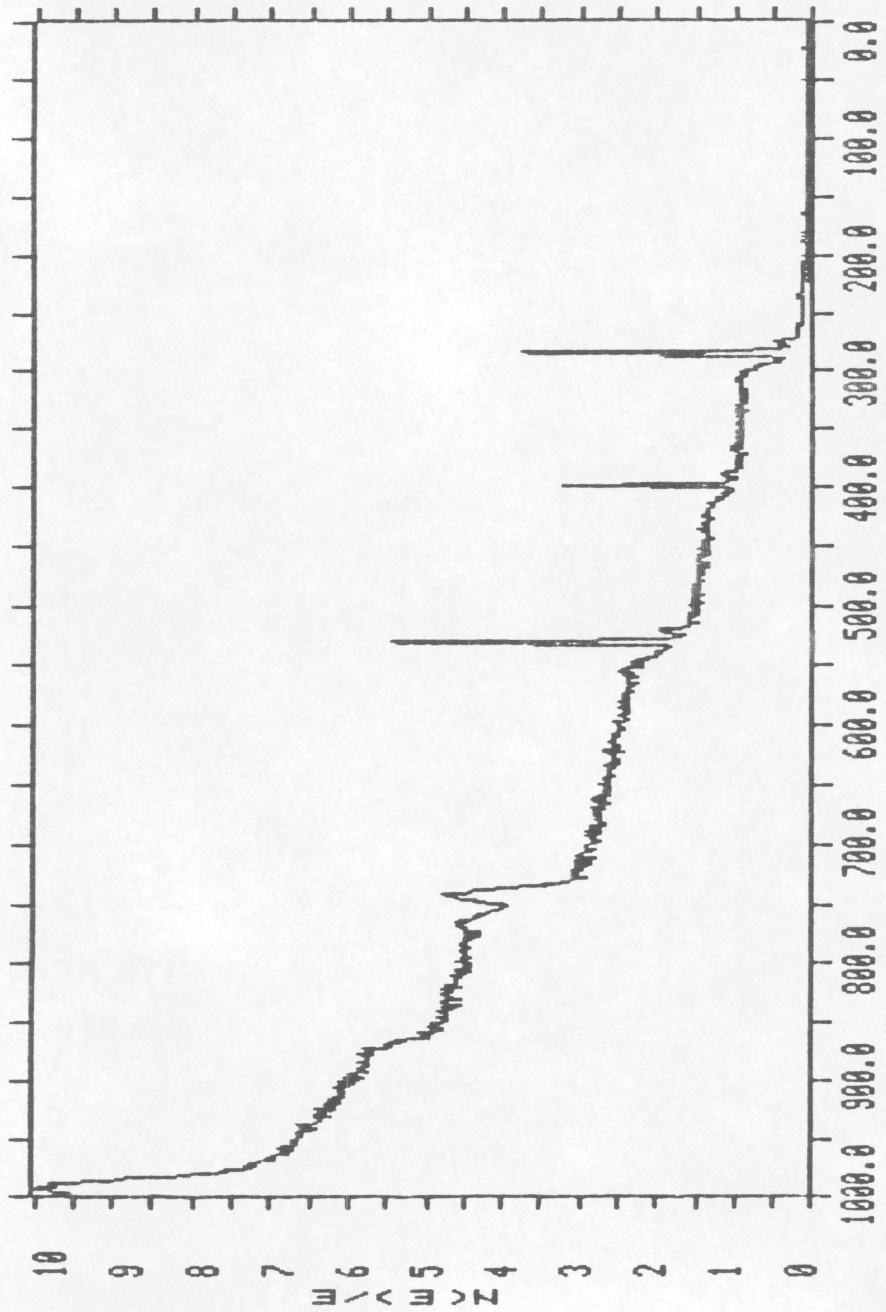

Figure 4.10. ESCA Spectrum of Poly-Sep AA 200.

TABLE 4.1

ESCA ANALYSIS OF ZEOLITES AND A POLYMER

Photopeak		NaY BE (eV)	NaY AF	5A BE (eV)	5A AF	ZSM-5 BE (eV)	ZSM-5 AF	Poly-Sep AA BE (eV)	Poly-Sep AA AF
Si	2p	102.8	0.17	102.0	0.13	103.1	0.22		
Al	2p	74.4	0.051	74.1	0.094	74.3	0.012		
O	1s	532.2	0.57	531.6	0.55	532.7	0.55	531.6	0.22
Na	1s	1073.4	0.12	1072.5	0.032	1072.9	0.036		
Ca	2p	347.4	0.001	348.0	0.021				
C	1s	285.0	0.085	285.0	0.17	285.0	0.18	285.0	0.62
N	1s							399.8	0.16

BE Binding Energy
AF Atomic Fraction

TABLE 4.2

COMPARISON BETWEEN SURFACE AND BULK ANALYSIS OF ZEOLITES

		NaY	5A	ZSM-5
Si/Al	Bulk	2.4	1.0	74.
	Surface	3.2	1.4	20.
Na/Al	Bulk	1.0	0.2	0.8
	Surface	2.4	0.3	3.1
2xCa/Al	Bulk		0.8	
	Surface		0.4	

hydrogen which is not detected by ESCA). The surface of the polymer particles shows about the same amount of carbon (see Table 4.1), but the oxygen composition is greater on the surface while the nitrogen composition is depleted on the surface with respect to the bulk composition, showing that the oxygen atoms are more preferentially oriented towards the surface.

4.5 *HEATS OF IMMERSION*

4.5.1 Effect of outgassing temperature

Figure 4.11 shows the specific heats of immersion of NaY and 5A zeolites in water as a function of outgassing temperature. It is evident that outgassing at low temperatures leads to low values of heats of immersion because the whole inner volume of the zeolite is not available for interacting with the immersion liquid molecules. Relatively high temperatures (> 250°C) are needed during the outgassing process for most of the water molecules to desorb from the zeolitic structure. An outgassing temperature of about 250 °C is needed for NaY and at least 350°C for 5A.

It is observed that the rate at which the heat of immersion increases with temperature is large initially and approaches zero at higher temperatures. Figure 4.11 also shows that NaY more readily desorbs water during the outgassing process than 5A does. The shape of the curve reflects the fact that 5A tends to bind water molecules more strongly than NaY since at low outgassing temperatures its heat of immersion in water is smaller because a large amount of water is still retained in the pores. But, at high outgassing temperatures the heat of immersion of 5A in water is larger than that of NaY reflecting its greater hydrophilicity.

The heat of immersion of NaY and 5A in water as a function of outgassing temperature confirms and supports the results of the TGA analysis (see section 4.1). Since TGA is easier to

perform, it is recommended that this technique be used in order to determine the outgassing temperature required for the calorimetric study.

Figure 4.12 gives the specific heat of immersion of NaY and 5A in water as a function of load fraction (coverage) of water. Load fraction is the ratio of the volume of liquid inside the pores of the zeolite to the total volume of the void space of the zeolite (maximum capacity). The load fraction of water on the zeolites was calculated in the following way: the residual amount of water in the zeolites at a given outgassing temperature was determined from the TGA diagrams; these values were divided by the maximum capacity for NaY and 5A of 0.34 and 0.28 cm^3/g, respectively.

The curves in Figure 4.12 reflect the affinity of these zeolites for water as suggested by the small drop of the heats of immersion even at relatively high loading fractions of 0.3 - 0.4. Curves of heats of immersion as a function of pre-adsorbed wetting liquid reported by Chessick and Zettlemoyer (62) show a rapid decrease of the heat of wetting with increasing coverage. Certainly the curves in Figure 4.12 do not correspond to any of the five types reported by these authors. An updated review of immersion calorimetry should include the type of curve shown in Figure 4.12.

Figures 4.13 and 4.14 show the effect of outgassing time and temperature respectively, on the specific heat of immersion of Poly-Sep AA 200 in water.

4.5.2 Effect of isomer bulk

Table 4.3 gives the specific heats of immersion of NaY and 5A in n-butanol and s-butanol. NaY has pores of 0.8 nm and therefore the heats of immersion in n-butanol and s-butanol are the same since both isomers can easily get into the super-cages of this zeolite. The specific immersion times are also short, consistent with a model of accessible pores as discussed below. In contrast, s-butanol, which is bulkier than n-butanol, is more restricted to enter in the α-cages of 5A which has an aperture of only 0.5 nm. Thus the heat of immersion is lower by 45% for s-butanol compared to n-butanol. The longer specific times of immersion are also consistent with

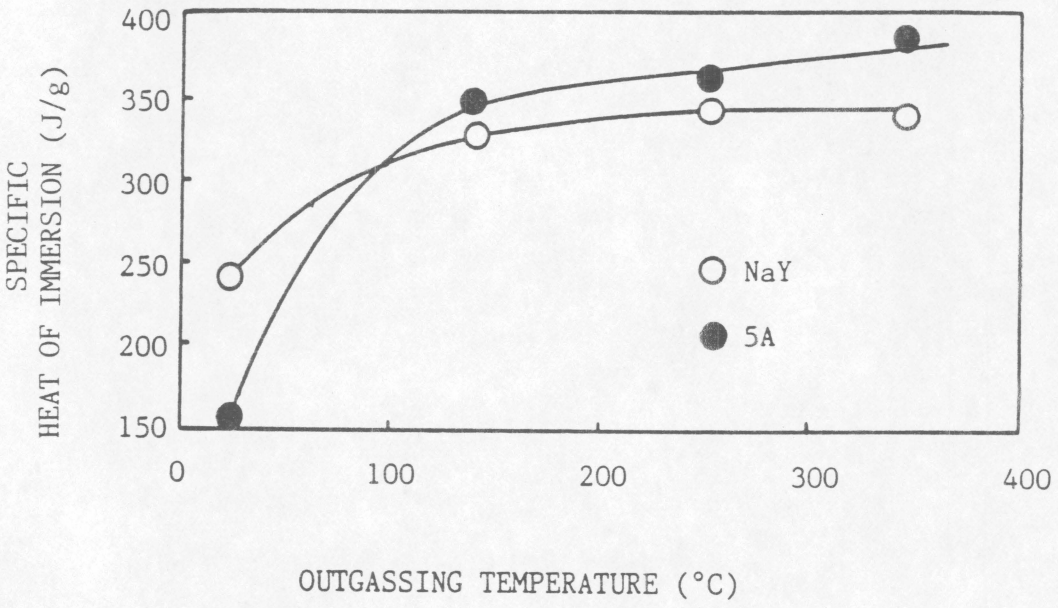

Figure 4.11. Effect of Outgassing Temperature on Heat of Immersion of Zeolites in Water.
Outgassing time: 24h

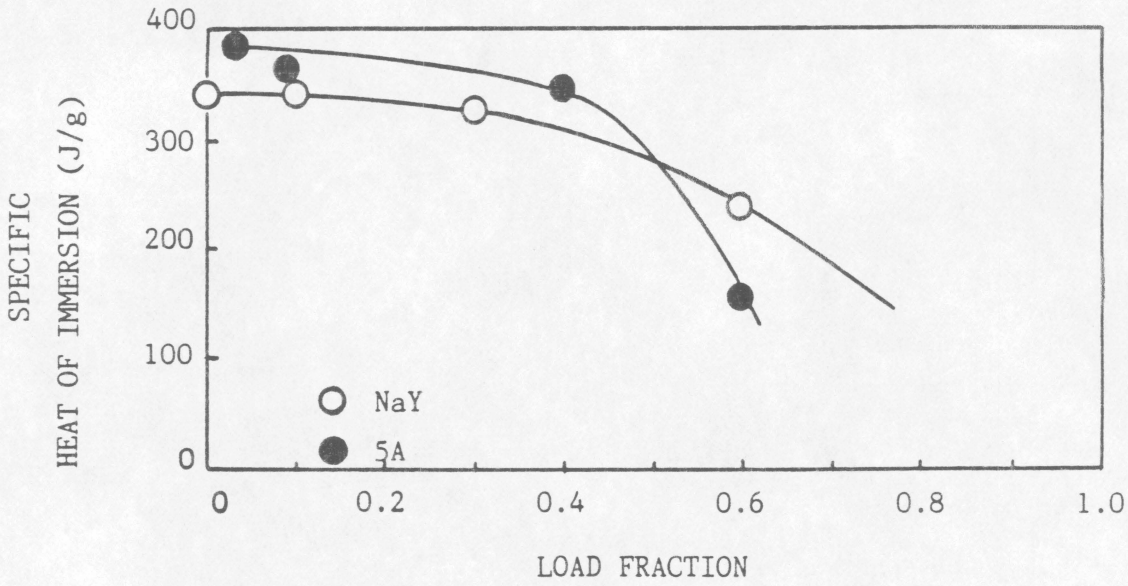

Figure 4.12. Specific Heat of Immersion of Zeolites in Water as a Function of Load Fraction.

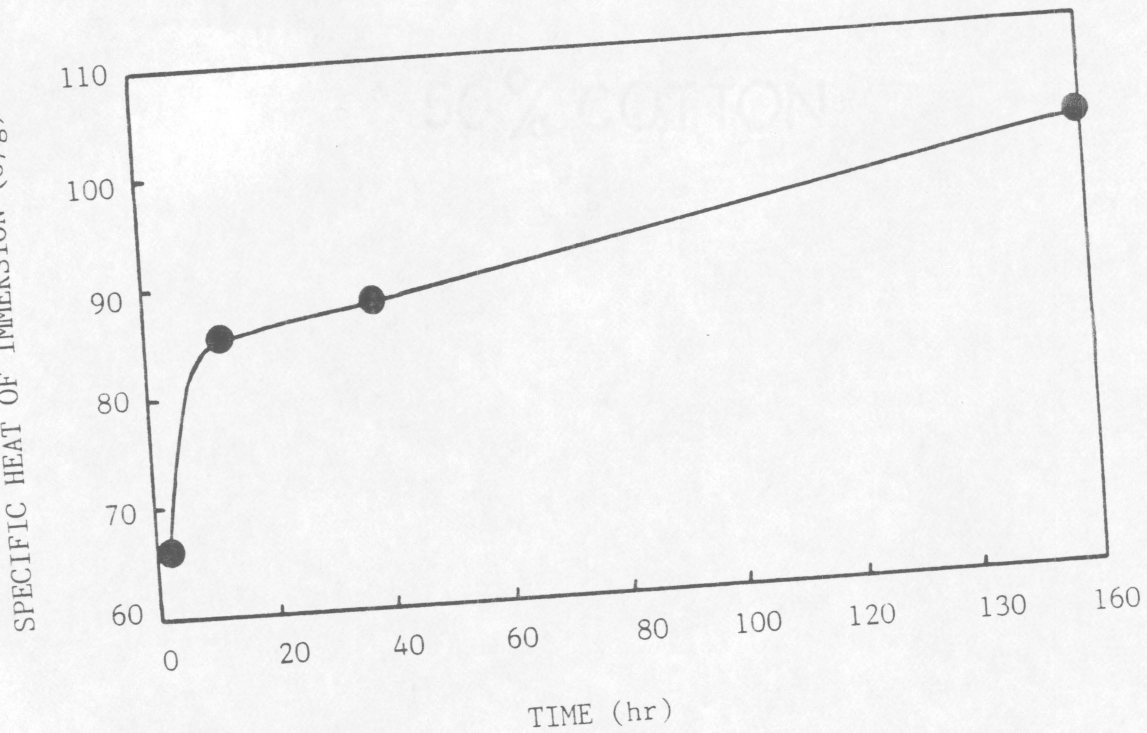

Figure 4.13. Effect of Outgassing Time on Heats of Immersion of POLY-SEP AA 200 in Water.

TABLE 4.3

HEATS OF IMMERSION OF NaY AND 5A IN BUTANOL ISOMERS

Liquid	Heat of Immersion (J/g)		Specific Time of Immersion (hr/g)	
	NaY	5A	NaY	5A
n-Butanol	202. ± 2.	252. ± 1.	1.1 ± 0.1	32. ± 1.2
s-Butanol	203. ± 5.	135. ± 29.	0.9 ± 0.0	14. ± 0.9

Outgassing Temperature = 142 °C
Outgassing Time = 24 hours

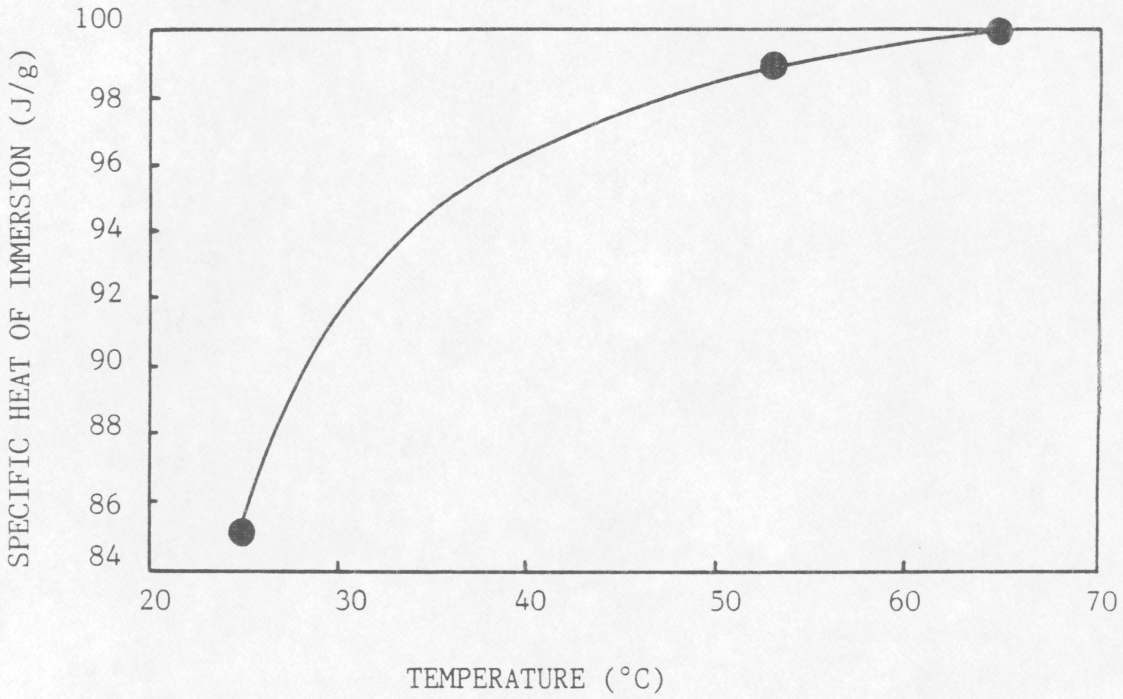

Figure 4.14. Effect of Outgassing Temperature on Heats of Immersion of POLY-SEP AA 200 in Water.

limited penetration by s-butanol. A portion of this heat must be due to the external surface of the crystals of 5A also.

4.5.3 Effect of number of carbon atoms of n-alcohol

The specific heats of immersion of NaY, 5A and ZSM-5 as a function of the number of carbon atoms in n-alcohols are given in Figure 4.15. First it is seen that the heats of immersion of 5A in n-alcohols are larger than those of NaY and ZSM-5, at least for the smaller alcohols. ZSM-5 shows the lowest values of heats of immersion. These results are consistent with the hydrophilic nature of 5A and NaY, 5A being more hydrophilic than NaY while ZSM-5 exhibits a rather hydrophobic behavior. It is also observed that the heats of immersion decrease non-linearly as the length of the n-alcohol chain increases for the zeolites NaY and 5A. This result suggests that as the chain length increases, the alcohol molecules become less and less accessible to the inner cavities of the zeolites. The decrease in heat also may be due to the fact that as the chain length of the alcohol molecules increases, there is a decrease in the concentration of OH groups per unit volume of alcohol adsorbed. It can be calculated from the density and the molecular weight of the alcohols that the concentration of OH groups for methanol is 0.0247 mole/cm^3 while for dodecanol the value is 0.0045 mole/cm^3. Thus, the OH concentration is more than 5 times lower for dodecanol than for methanol. However, the heat of immersion of NaY in dodecanol is less than twice that of NaY in methanol. Hence, not only are the OH groups responsible for the heat of immersion, but also the CH_2 and CH_3 groups must contribute to the total heat of immersion due to dispersion forces. In fact, it has been shown that heats of immersion of X type zeolite, which is similar to Y type in structure but with a higher Al content, in liquids such as methanol and methylamine, can be approximately calculated by the summation of all the contributions of the different groups that interact with the structure either specifically or non-specifically (75).

In contrast, ZSM-5 exhibits an increase in heats of immersion as a function of chain length up to n-pentanol and then a decrease for longer alcohols. This result can be interpreted in terms

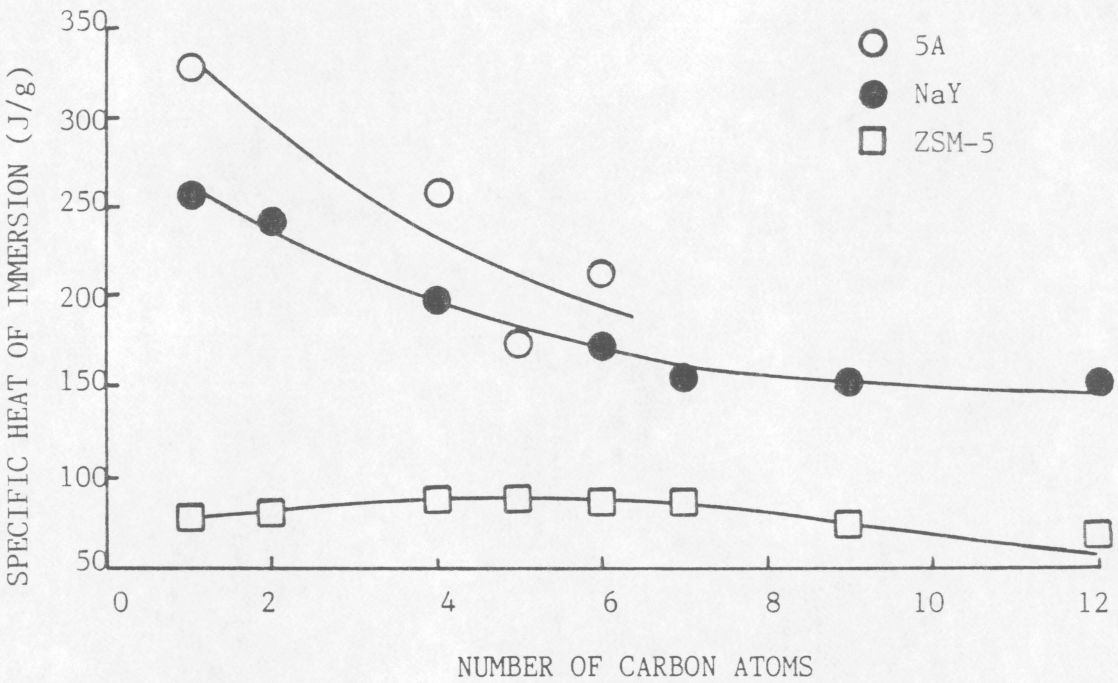

Figure 4.15. Specific Heats of Immersion of Zeolites in n-alcohols.

of the hydrophobic nature of ZSM-5. As the number of carbons in the alcohols is increased, the hydrocarbon portion of the alcohol becomes longer leading to increased dispersion force interacting with the hydrophobic zeolite. But when the hydrocarbon portion of the alcohol becomes too long, the accessibility of the alcohol molecules to the pores of ZSM-5 becomes limited leading to a decrease in the heat of immersion.

Figures 4.16, 4.17 and 4.18 give the specific heat of immersion of NaY, 5A and ZSM-5 in n-alcohols re-plotted on different scales showing the errors associated with the measurements. Generally the errors tended to be larger for higher alcohols probably because the immersion times were longer and the calorimeter showed some instability and drifting of the base line over long equilibration periods of running time.

Figure 4.19 gives a comparison between heats of immersion of NaY in n-alcohols reported recently by Messow, et al. (69) and the present results. It is seen that the present results are in agreement with those of Messow. The difference in Si/Al ratio of both zeolites is small, the zeolite used in this work has a slightly higher aluminum content (Si/Al = 2.4) and so a higher sodium concentration than that of zeolite NaY used by Messow (Si/Al = 2.6). It is known that zeolites with a higher Al content are more hydrophilic due to the higher cation concentration in the cavities. Chen (76) has recently reported that the behavior of hydrophilic zeolites can be reversed by removing aluminum and thereby cations from the structure. This is probably the main reason for 5A being the most hydrophilic and ZSM-5 the most hydrophobic (see Table 4.2). Therefore, variations in the Si/Al ratio for zeolites are responsible for changes in hydrophilicity and thus in heats of immersion.

Figure 4.20 is a clearer illustration of the effect of the Si/Al ratio on heats of immersion of ZSM-5 in n-alcohols. A comparison is given of heats of immersion for ZSM-5 with a Si/Al ratio of 74 used in this work and literature values (69) for ZSM-5 with a Si/Al ratio of 24 and silicalite, which is a molecular sieve with the same structure as ZSM-5 but without any aluminum atoms in its framework (54). It is observed that there is a large increment in heats of immersion with increasing Al content for the smaller alcohols. This gap being smaller as chain length is increased, with all the molecular sieves approaching the same value for the higher alcohols in the series.

The large difference in heats of immersion that is observed for the small alcohols is obviously due to the difference in the aluminum content of the zeolite that creates charge sites in the structure which are balanced by cations. These sites and the cations will interact strongly with the polar group of the wetting alcohol molecules. The long hydrophobic portion of the large alcohols predominates over the polar group and will interact rather with the rest of the structure of the molecular sieve which is hydrophobic also. The same limiting value is reached since there is not much variation in the structure itself because only 1 and 3 silicon atoms out of every 75 have been replaced by aluminum atoms in the ZSM-5 used in this work and the one used by Messow, respectively. The fact that the zeolite ZSM-5 used in the present work in which some protons have been replaced by sodium ions and that used by Messow which is supposed to contain only protons, do not have the same type of cations may have contributed to the difference of the heat of immersion values. Although, the aluminum concentration and so the cation concentration appears to be the predominant factor since silicalite that has no aluminum content shows the least heat of immersion value. Figure 4.21 shows the same information as Figure 4.20, but the Al/Si ratio axis is added, so a three dimensional surface is presented.

Poly-Sep AA did not give any significant amount of heat compared to the heat of empty bulb when immersed in alcohols. In contrast, the heat of immersion of Poly-Sep AA in ethylene glycol was high; but the time required for this process was very long (4-5 days) so it was not possible to do further experimentation with this polymer.

4.6 KINETICS OF IMMERSION

The time required for re-attaining steady state in the calorimeter after breaking the bulb tip is the time of immersion. The specific time of immersion is defined as the immersion time per unit mass of sample (see section 3.2.3).

The specific time of immersion 't_s' was calculated using the following expression:

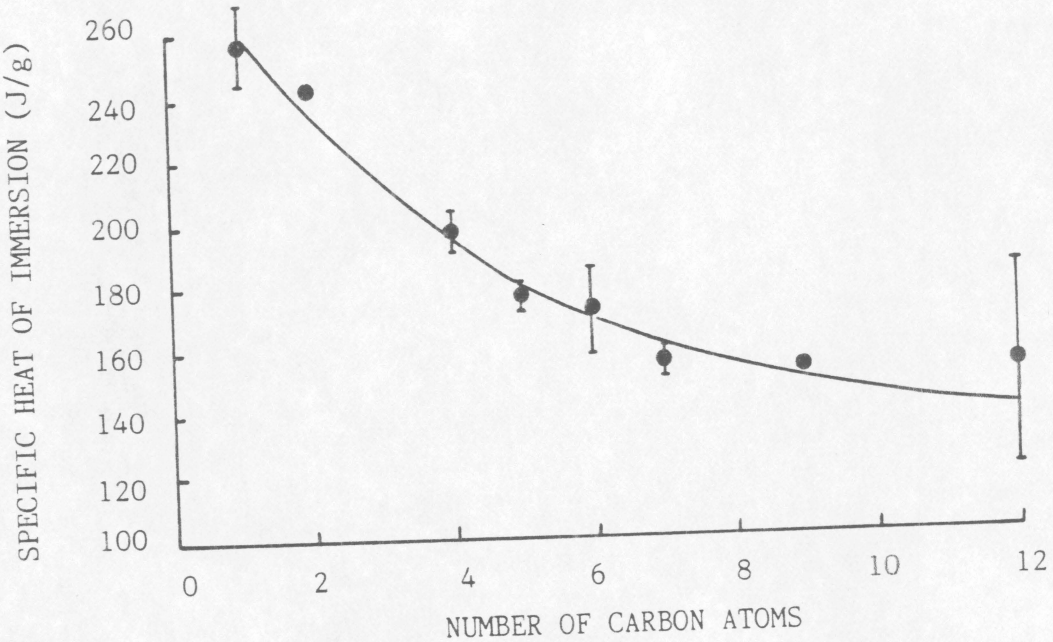

Figure 4.16. Specific Heat of Immersion of NaY in n-alcohols.

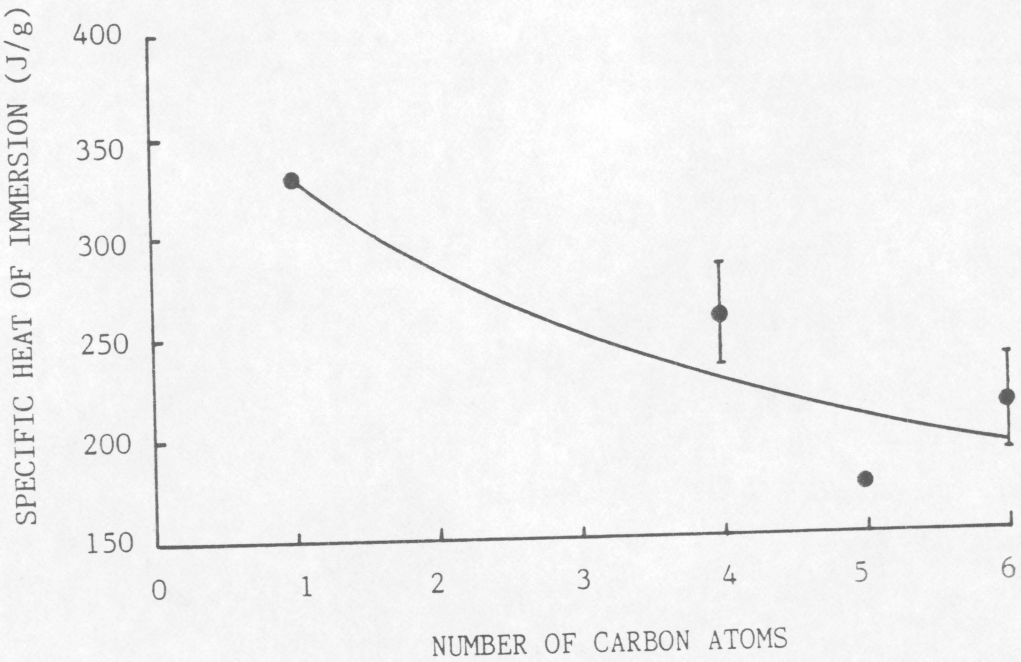

Figure 4.17. Specific Heats of Immersion of 5A in n-alcohols.

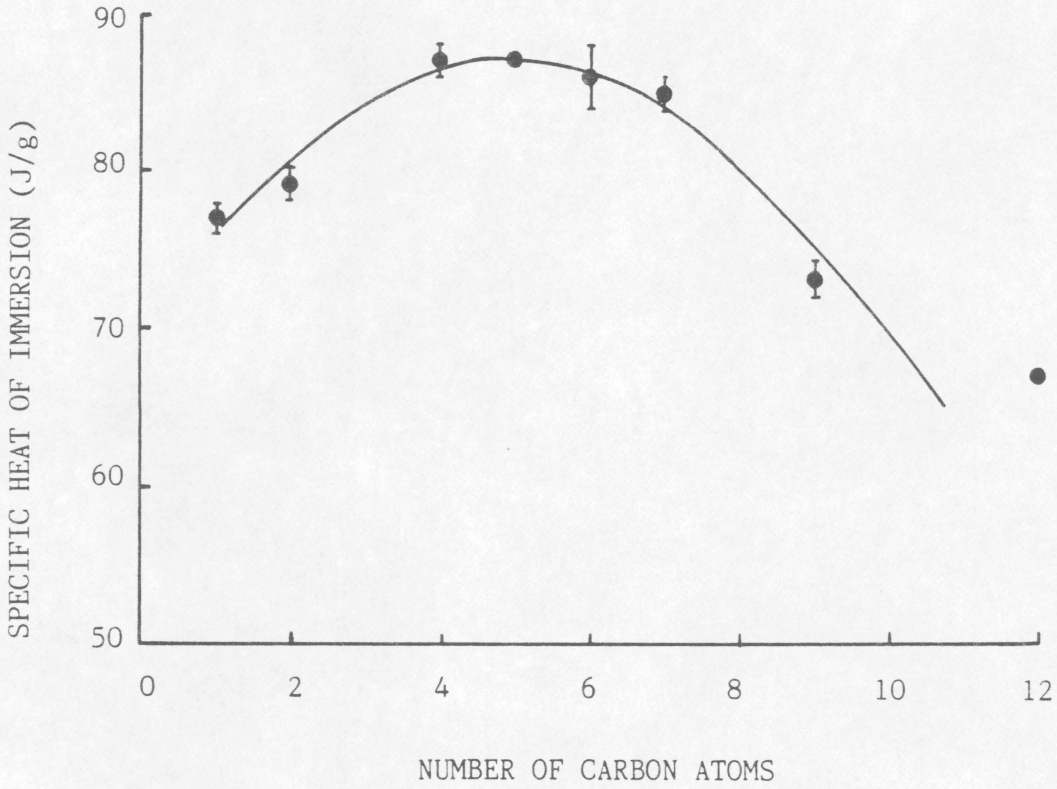

Figure 4.18. Specific Heats of Immersion of ZSM-5 in n-alcohols.

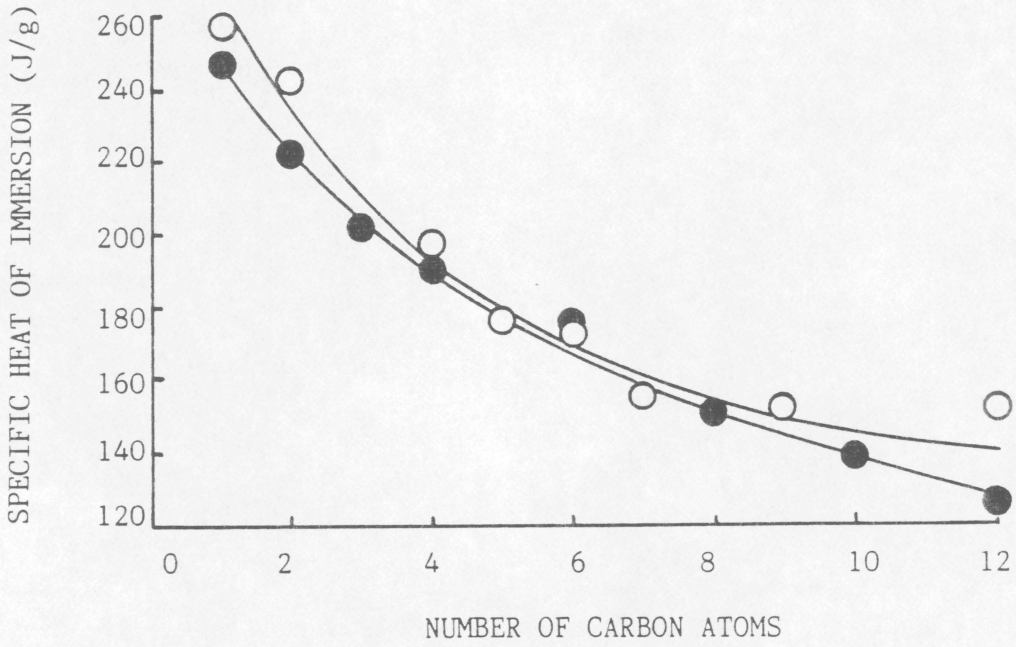

Figure 4.19. Specific Heat of Immersion of NaY in n-alcohols.
○ Present Values; ● Literature Values (69)

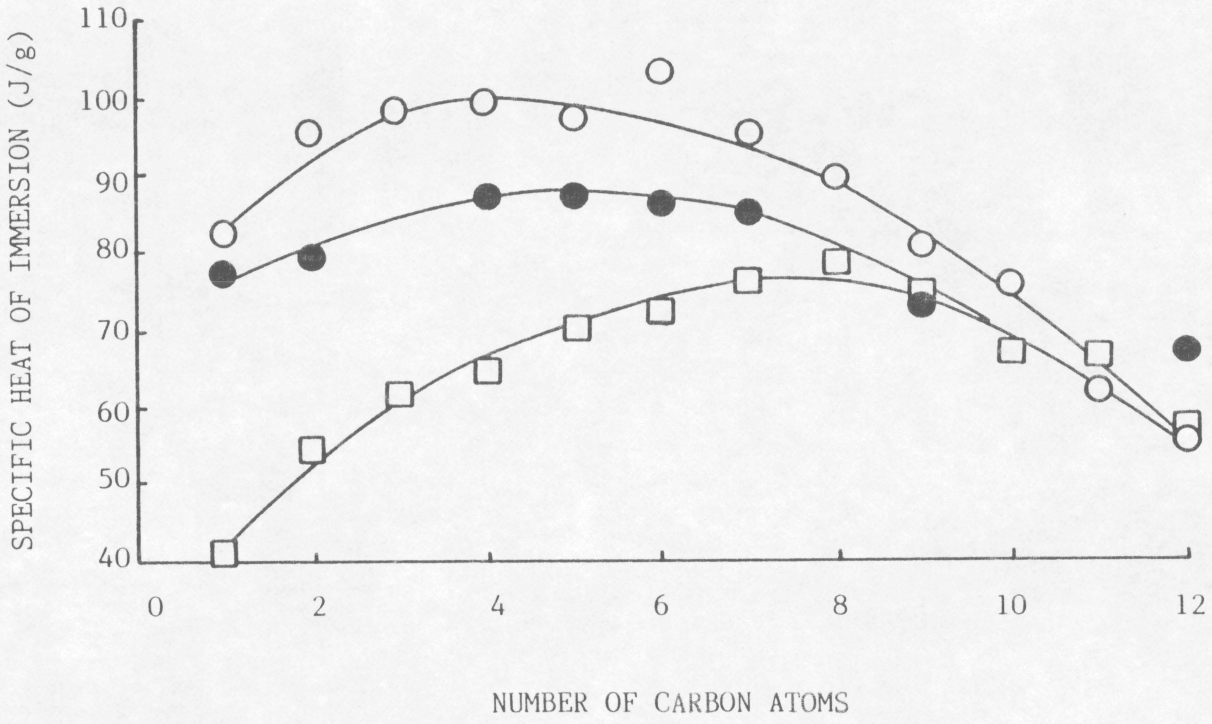

Figure 4.20. Specific Heat of Immersion of ZSM-5 and Silicalite in n-alcohols.

○ H-ZSM-5(Si /Al = 24) (69) ● ZSM-5 (Si/Al = 74)(Present Values);
□ Silicalite (69).

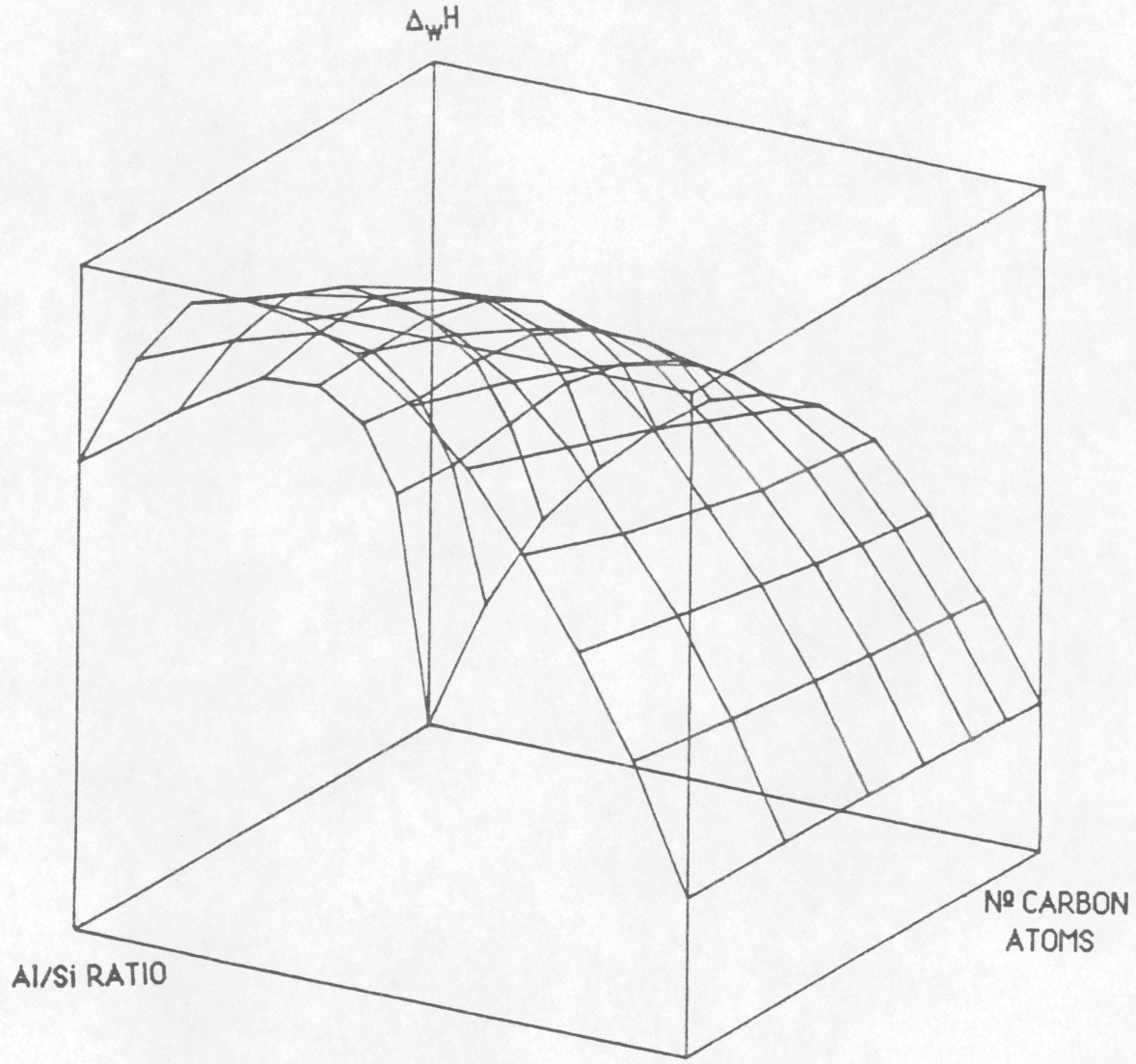

Figure 4.21. Specific Heats of Immersion of ZSM-5 with Different Al/Si Ratios in n-alcohols.

$$t_s = t \frac{\ln(C_t/W)}{lnC_t} \quad (4.1)$$

where 'C_t' is the total calorimeter counts, 'W' is the weight of the sample used and 't' is the equilibration time. Equation 4.1 can be derived from the fact that'C' is proportional to 'W' and assuming that 't' is proportional to ln C. In other words, the immersion process is assumed to follow first order kinetics as discussed below.

Figure 4.22 shows the specific time of immersion as a function of number of carbon atoms of alcohol. NaY exhibits a very poor linear correlation (least squares method) with a regression coefficient of 0.10 and a slight increase in time of 0.01 hours per carbon atom per gram of sample. The average specific time is 1.2 hr/g. This result is consistent with the conclusion that all the alcohol molecules readily penetrate the large pores of NaY in a relatively short time.

Zeolite 5A also shows a relatively poor linear correlation with a regression coefficient of 0.44 and an increase of 1.46 hours per carbon atom per gram of sample. It is evident that penetration of the larger alcohol molecules is more restricted into the pores of 5A, taking a long time to diffuse into them. ZSM-5 presents a good linear correlation with a regression coefficient of 0.94 and an increase of 0.4 hours per carbon atom and per gram of sample. This zeolite exhibits an intermediate behavior in alcohol penetration since the pore aperture is between that of NaY and ZSM-5. Since large uncertainties (up to 64%) were involved in the measurements of the times of immersion, the results should be taken more as semi-quantitative rather than as quantitative.

Calorimetric counts (proportional to heat) as a function of time appear to follow first order kinetics. A plot of ln (C_t - C) as a function of time (t) should be a straight line of slope equal to the negative of the first order rate constant 'k'; 'C_t' is the total calorimetric counts when the process of heat release is complete and therefore steady state is re-attained; 'C' is the calorimetric counts at any time (t) during the process.

Figure 4.23 shows a plot of $\ln(C_t - C)/\ln C_t$ as a function of time for various systems immersed in water; Figures 4.24, 4.25 and 4.26 give the same type of plots for the immersion of NaY, 5A and ZSM-5 in n-alcohols, respectively. The quantity $\ln(C_t - C)$ has been divided by

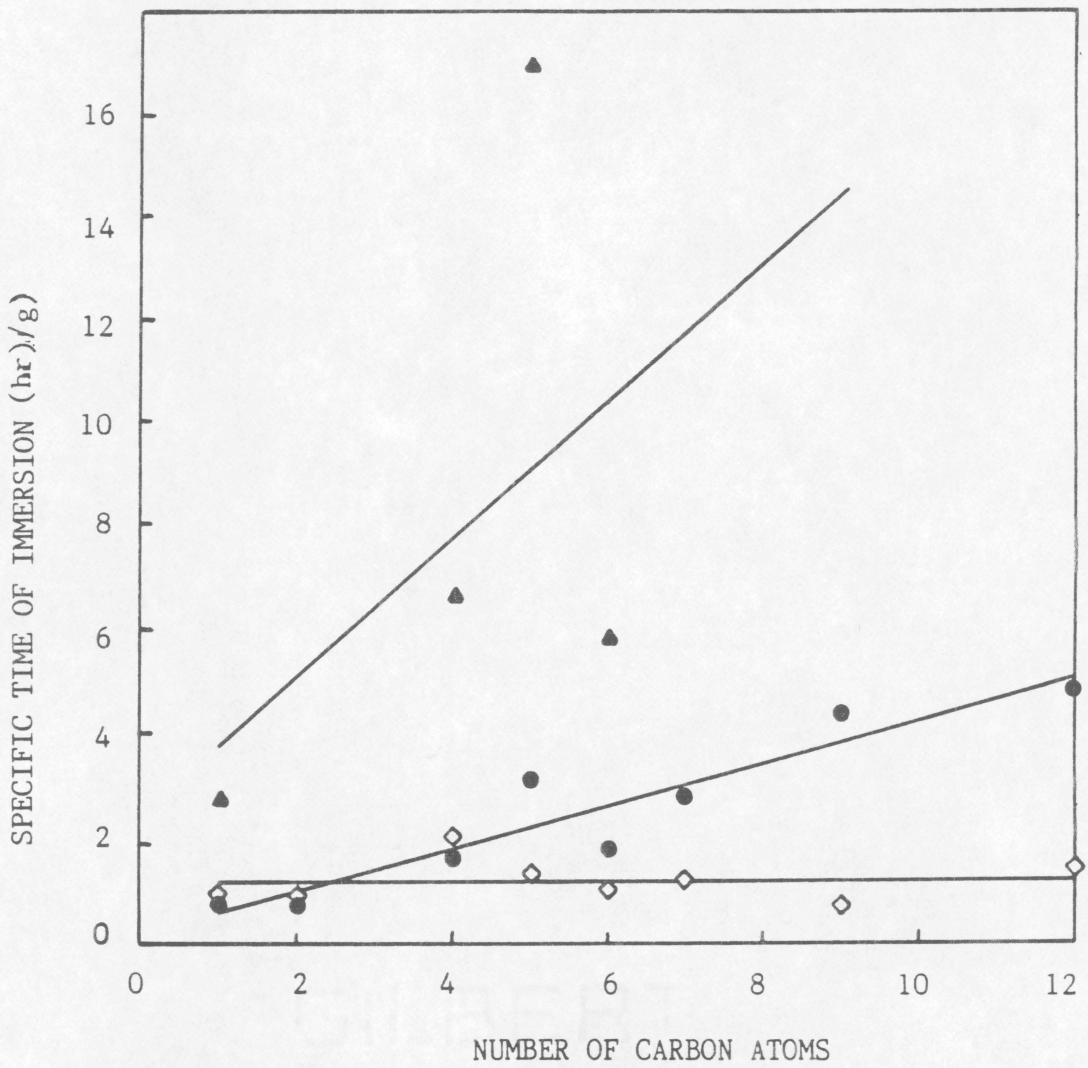

Figure 4.22. Kinetics of Immersion of Zeolites in n-alcohols.

◇ NaY

● ZSM-5

▲ 5A

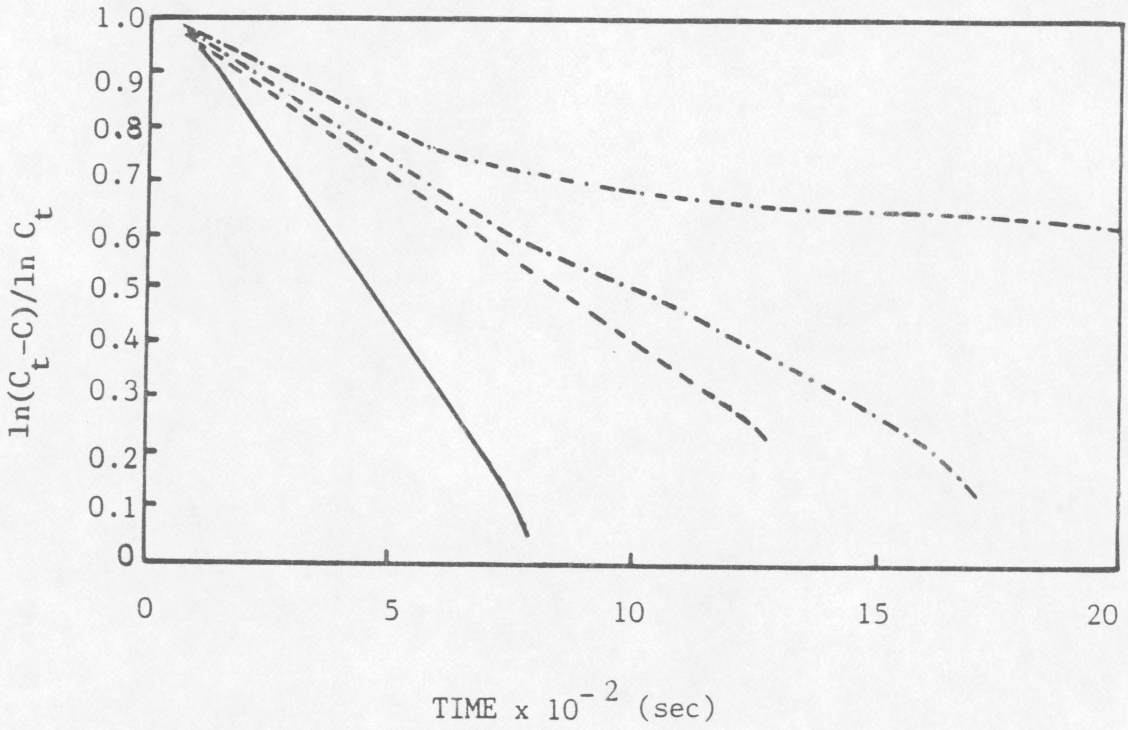

Figure 4.23. First Order Kinetic Plots for Various Systems in Water.

——— Empty Bulb

– – – – Poly Sep AA200

·–·–·– ZSM-5

·– – ·– – NaY

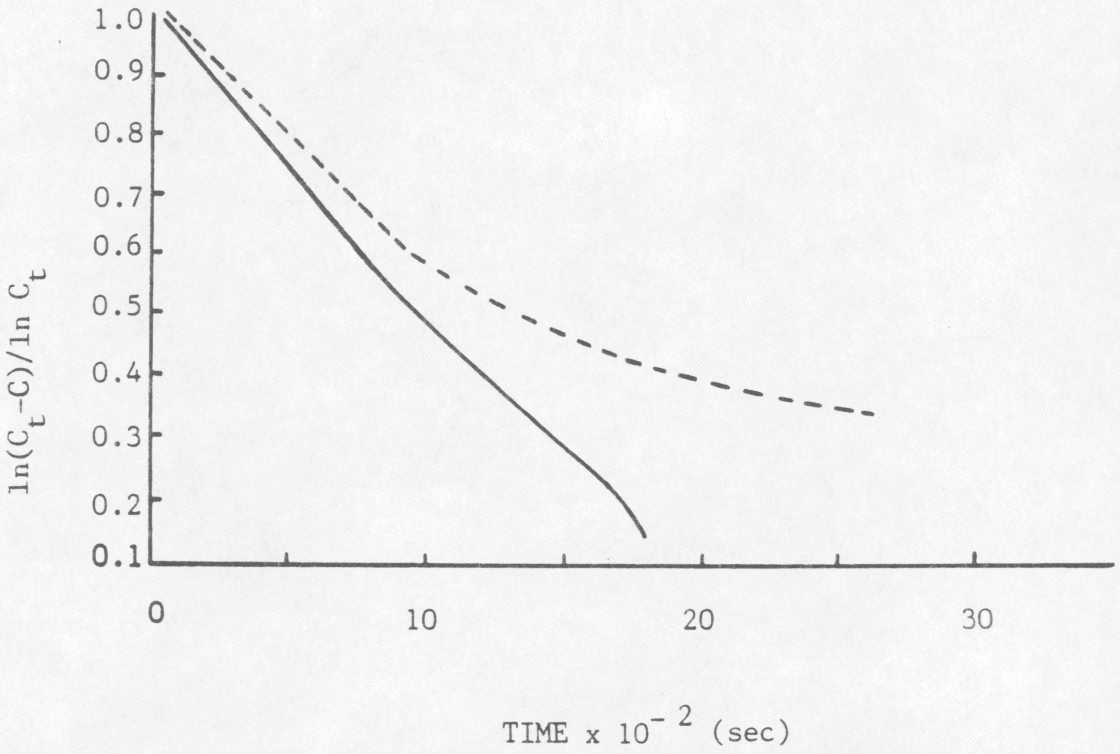

Figure 4.24. First Order Kinetic Plots for the Immersion of NaY in n-alcohols

——— Methanol

- - - - n-Butanol

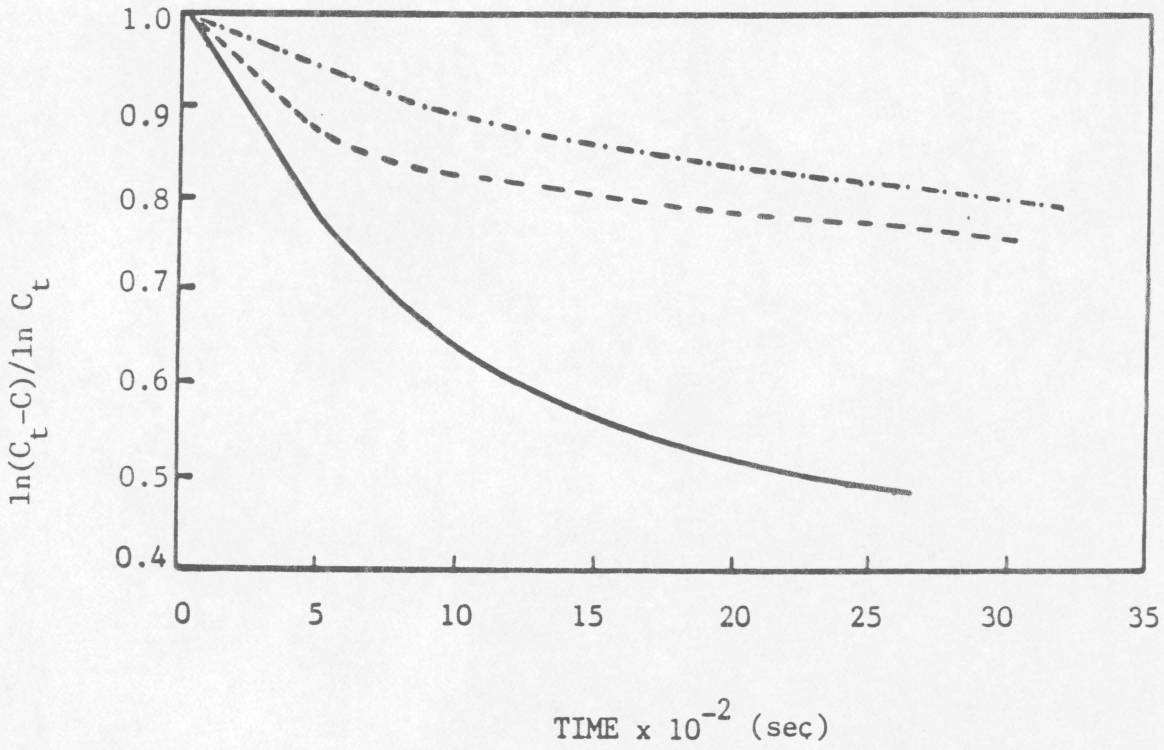

Figure 4.25. First Order Kinetic Plots for the Immersion of 5A in n-alcohols.

——— Methanol

– – – – n-Butanol

– · – · – n-Hexanol

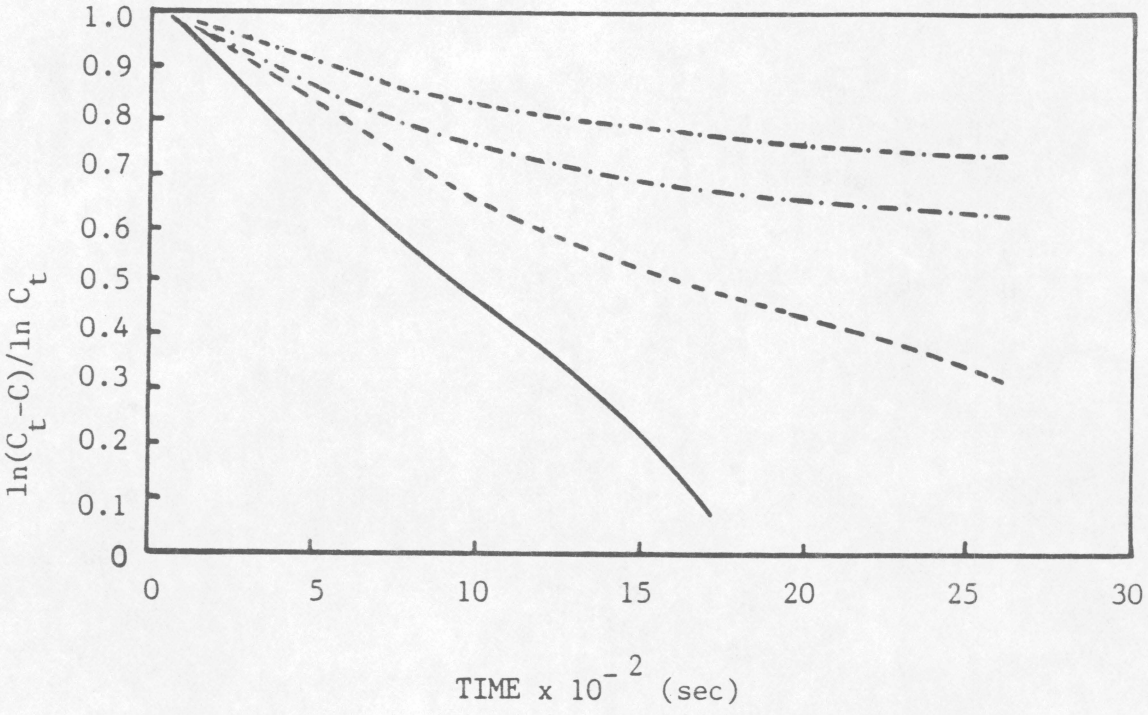

Figure 4.26. First Order Kinetic Plots for the Immersion of ZSM 5 in n-alcohols.

——— Methanol

– – – – n-Butanol

·—·—· n-Heptanol

·——·—— n-Nonanol

$\ln C_t$ just for convenience since in this way all the systems are on the same ordinate scale from 0 to 1 making a visual comparison of the different curves easier. However, the slopes of the linear portions of the curves of Figure 4.23 and subsequent figures were calculated from the original plot of $\ln(C_t - C)$ Vs t. A straight line is observed for the process of breaking an evacuated empty bulb. Since the release of mechanical heat due to the breakage and suction of the liquid into the bulb is practically instantaneous, actually what is observed over the 750 second time period is the heat transfer through the cylindrical stainless steel cell which follows first order kinetics. The small deviation from linearity at the beginning of the line must be due to a short delay of response due to the time constant of the entire system: bulb - liquid - cell. If the heat release during the immersion process were instantaneous, lines with the same slope and equal to that for the empty bulb would have been observed for all systems. Actually different slopes were observed for the different solids used and thus there is a time dependence involved in the process of immersion of solids in liquids which may be different for each system.

An overall rate constant can be calculated for the immersion process but one cannot discriminate between the kinetics of the immersion process itself and the heat transfer kinetics. Apparently the immersion process is faster than or comparable to the heat transmission process. For the immersion of zeolites in water as well as in alcohols as seen in Figures 4.24, 4.25 and 4.26, a linear portion is observed initially and then deviation from linearity at longer times. It is important to note that more than 80% of the total heat is released withi n the linear portion. Thus some heat is released relatively slowly, this effect being more pronounced as the alcohol gets larger and as the pore size of the zeolite gets smaller. Table 4.4 gives the overall rate constants associated with the linear portion of the plots for the immersion of the zeolites in water and alcohols.

The rate constant for NaY does not vary with the liquid used and this constancy is consistent with unrestricted access of the liquid molecules into the pores. There is a definite lowering of the rate constant for ZSM-5 as the alcohol molecules become bulkier. This decrease in rate constant is consistent with limited accessibility of the larger alcohols. A similar trend is observed for 5A.

TABLE 4.4

OVERALL RATE CONSTANT OF IMMERSION OF ZEOLITES IN WATER AND n-ALCOHOLS

	Zeolite		
	NaY	5A	ZSM-5
Liquid	$k \times 10^3$ (sec^{-1})	$k \times 10^3$ (sec^{-1})	$k \times 10^3$ (sec^{-1})
Water	3.6	-	3.9
Methanol	4.5	3.8	4.5
Ethanol	4.5	-	4.5
n-Butanol	3.7	1.7	3.1
n-Pentanol	3.8	-	-
n-Hexanol	-	1.1	3.1
n-Heptanol	3.6	-	2.5
n-Nonanol	3.7	-	2.3
n-Dodecanol	3.8	-	1.5

Chapter V

SUMMARY

The research concerning the interactions of zeolites NaY, 5A and ZSM-5 with liquids is summarized below. Heats and kinetics of immersion of zeolites in dry n-alcohols provided information about the accessibility of the alcohol molecules into the pores of the zeolites and a measure of the strength of the interaction between alcohols and the zeolites given by the magnitude of the heats of immersion. The specific heat of immersion in alcohols and water was in the order of 5A > NaY > ZSM-5 due to the hydrophilicity of those zeolites that is in the same order. The specific heats of immersion decreased non-linearly as the length of the alcohol molecule increased for zeolites NaY and 5A which can be rationalized in terms of molecular accessibility to the pores of these zeolites. The longer the chain length of alcohol, the less accessible it is to the pores of a given zeolite. The accessibility is more limited for the zeolites with smaller pore diameters. In contrast, the specific heats of immersion as a function of number of carbon atoms of alcohol for ZSM-5 showed an increase initially up to n-pentanol and then a decrease for longer alcohols. This result can be interpreted in terms of the hydrophobic nature of ZSM-5. As the chain length of the alcohol increases, the hydrocarbon portion of the alcohol becomes longer leading to an increase of the dispersion forces interacting with the hydrophobic structure, but when the alcohol molecule

becomes too long, its accessibility to the pores of the zeolite becomes the limitation, consequently a decrease of the specific heat of immersion results. The heats of immersion in alcohols obtained for ZSM-5 were compared with similar results found in the literature for a ZSM-5 with a higher Al/Si ratio and with silicalite which has no aluminum at all. The comparison suggests that the heats of immersion increase as the Al content and therefore the cation concentration increases in the zeolite. Althogh,the type of cation may also affect the magnitud of the heat of immersion.

The kinetic study of the immersion process confirms that the accessibility of the alcohol molecules to the pores of the zeolites is in the order of NaY > ZSM-5 > 5A. NaY showing almost no restriction for all the alcohols used since the specific immersion time showed almost no change with the number of carbon atoms in the alcohol, while ZSM-5 showed an increase of 0.4 hr/carbon atom and 5A 1.5 hr/carbon atom. In addition, it was determined that the overall process followed first order kinetics. The overall rate constants were determined. However, it must be stressed that it was not possible to study the kinetics of immersion without being affected by the heat transfer kinetics of the calorimetric cell.

REFERENCES

1. Gottardi, G., and Galli, E., "Natural Zeolites" Springer-Verlag, Berlin Heidelberg (1985).
2. Breck, D.W., "The Properties and Applications of Zeolites," (R. P. Townsend, Ed.) The Chemical Society, Special Publication No 33, London, 1979, p.391
3. Way, J. T., J. Roy. Agr.Soc. 11, 313 (1850).
4. Flanigen, E.M., "Proceed. 5th. Internat. Confer. on Zeolites," (L. V. C. Rees, Ed.), Heyden, London, 1980.
5. Glanville, J.O., and Wightman, J.P., Fuel 59, 561 (1980).
6. Widyani, E., Wightman, J.P., Colloids and Surfaces 4, 209 (1982).
7. Newcomb, K.L., Thesis, VPI & SU, Blacksburg, VA (1984).
8. Phillips, K. M., Glanville, J. O., and Wightman, J. P., Colloids and Surfaces 21, 1 (1986).
9. Glanville, J. O., Newcomb, K. L., and Wightman, J. P., Fuel 65, 485 (1986).
10. Breck, D.W., "Zeolite Molecular Sieves", John Wiley, New York (1974).
11. Breck, D.W., "Molecular Sieve Zeolites", (R. F. Gould, Ed.), Advan. Chem. Ser. 101,American Chemical Society, Washington, D. C., 1971, p.1
12. Sand, L.B., "Proceed. 5th Internat. Confer. on Zeolites", (L.V.C. Rees, Ed.), Heyden, London, 1980, p.1
13. Flanigen, E.M., "Molecular Sieves", (R. F. Gould, Ed.), Advan. Chem. Ser. 121, American Chemical Society, Washington, D. C., 1973, p.119
14. Flanigen, E.M., and Khatami, H., "Molecular Sieve Zeolites," (R. F. Gould, Ed.), Advan. Chem. Ser. 101, American Chemical Society, Washington, D. C., 1971, p.201
15. Ward., J.W., "Molecular Sieve Zeolites," (R. F. Gould, Ed.), Advan. Chem. Ser. 101, American Chemical Society, Washington, D. C., 1971, p.380
16. Zhdanov, S.P., Kiselev, A.V., Ligin, V.I., and Titova, T.I., Russ. J. Phys. Chem. 38, 1299 (1964).

17. Kiselev, A.V., Kubelkova, L., and Lygin, V.I., Russ. J. Phys Chem. 38, 1480 (1964).

18. Brodskii, I.A., and Zhdanov, S.P., "Proceed. 5th. Internat. Confer. on Zeolites," (L.V.C. Rees, Ed.), Heyden, London, 1980, p.234

19. Maiwald, W., Basler, W.D., and Leckert, H.T., "Proceed. 5th Internat. Confer. on Zeolites," (L.V.C. Rees, Ed.),Heyden, London, 1980, p.562

20. Basler, W.D., "Molecular Sieves," (R. F. Gould, Ed.), ACS Symposium Ser. 40, American Chemical Society, Washington, D. C., 1977, p.335

21. Resing, H.A., and Murday, J.S., "Molecular Sieves," (R. F. Gould, Ed.), Advan. Chem. Ser. 121, American Chemical Society, Washington, D. C., 1973, p.414

22. Fyfe, C.A., Gobbi, G.C., Hartman, J.S., Klinouski, J., and Thomas, J.M., J. Phys. Chem. 86, 1247 (1982).

23. McMillan, M., Brinen, J.S., and Haller, G.L., J. Catal. 97, 243 (1986).

24. Thomas, J.M., Klinowski, J., Fyfe, C.A., Gobbi, G.C., Ramadas, S., and Anderson, M.W., "Intrazeolite Chemistry," (M. J. Comstock, Ed.), ACS Symposium Ser. 218, American Chemical Society, Washington, D. C., 1983, p.159

25. Tempere, J., Delafosse, D., and Cantour, J.P., "Molecular Sieves," (R. F. Gould, Ed.), ACS Symposium Ser. 40, American Chemical Society, Washington, D. C., 1977, p.76

26. Defosse, C., Delmon, B., and Canesson, P., "Molecular Sieves," (R. F. Gould, Ed.), ACS Symposium Ser. 40, American Chemical Society, Washington, D. C., 1977, p.86

27. Klug, H.P., and Alexander, L.E., "X-Ray Diffraction Procedures", John Wiley, New York, 1954.

28. Jarman, R.H., Zeolites 5, 213 (1985).

29. Johari, O., and Samudra, A.V., "Characterization of Solid Surfaces", P. Krane and G.B. Larrabee, Plenum Press, New York, 1974.

30. Aznarez, J.A., Garcia, M.A., Mendioroz, S., and Pajares, J.A., Rev. Real Acad. Ciencias Exact. Fis. Nat. (Madrid) 79, 289 (1985).

31. Thomas, J.M., Millward, G.R., and Ramadas, S., "Intrazeolite Chemistry," (M. J. Comstock, Ed.), ACS Symposium Ser., 218, American Chemical Society, Washington, D. C., 1983, p.181

32. Li, C.Y., and Rees, L.V.C., Zeolites 6, 217 (1986).

33. Lygin, V.I., "Molecular Sieve Zeolites," (R. F. Gould, Ed.), Advan. Chem. Ser. 102, American Chemical Society, Washington, D. C., 1971, p.86

34. Jacobs, P.A., "Carboniogenic Activity of Zeolites", Elsevier, Amsterdam (1977).

35. Brunauer, S., Emmett, P.H., and Teller, E., J. Amer. Chem. Soc. 60, 309 (1938).

36. McClellan, A.L., and Harnsberger, H.F., J. Colloid Interface Sci. 23, 577 (1967).

37. Stakebake, J.L., and Fritz, J., J. Colloid Interface Sci. 100, 33 (1983).

38. Suzuki, I., Oki, S., and Namba, S., J. Catal. 100, 219 (1986).

39. Kiselev, A.V., "Molecular Sieve Zeolites," (R. F. Gould, Ed.), Advan. Chem. Ser., 102, American Chemical Society, Washington, D. C., 1971, p.37

40. Carter, J.W., "The Properties and Applications of Zeolites," (R. P. Townsend, Ed.) The Chemical Society, Special Publication No 33, London, 1979, p.76

41. Lee, H., "Molecular Sieves," (R. F. Gould, Ed.), Advan. Chem. Ser., 121, American Chemical Society, Washington, D. C., 1973, p.311

42. Sherry, H.S., "Molecular Sieve Zeolites," (R. F. Gould, Ed.), Advan. Chem. Ser., 101, American Chemical Society, Washington, D. C., 1971, p.350

43. Rabo, J. A., and Poutsma, M. L., "Molecular Sieve Zeolites," (R. F. Gould, Ed.), Advan. Chem. Ser. 102, American Chemical Society, Washington, D. C., 1971, p.284

44. Venuto, P.B., "Molecular Sieve Zeolites," (R. F. Gould, Ed.), Advan. Chem. Ser., 102, American Chemical Society, Washington, D. C., 1971, p.260

45. Vaughan, D.E.W., "The Properties and Applications of Zeolites," (R. P. Townsend, Ed.) The Chemical Society, Special Publication No 33, London, 1979, p.294

46. Csicsery, S.M., Zeolites 4, 202 (1984).

47. Eulenberger, G.R., Shoemaker, D.P., and Keil, J.G., J. Phys. Chem. 71,1812 (1967).

48. Breck, D.W., Eversole, W.G., Milton, R.M., Reed, T.B., and Thomas, T.L., J. Am. Chem. Soc. 78, 5963 (1956).

49. Reed, T.B., and Breck, D.W., J. Am. Chem. Soc. 78, 5972 (1956).

50. Broussard, L., and Shoemaker, D.P., J. Am. Chem. Soc. 82, 1041 (1960).

51. Yanagida, R.Y., Amaro, A.A., and Seff, K, J. Phys. Chem. 77, 805 (1973).

52. Kokotailo, G.T., Lawton, S.L., Olson, D.H., and Meyer, W.M., Nature 272, 437 (1978).

53. Chang, C.C., and Silvestri, A.J., J. Catal. 47, 249 (1977).

54. Flanigen, E.M., Bennett, J.M., Grose, R.W., Cohen, J.P., Patton, R.L., and Kirchner, R.M., Nature 271, 512 (1978).

55. Hemminger, W., and Holne, G., "Calorimetry Fundamentals and Practice", Verlag Chemie, Weinheim 1984.

56. Partyka, S., Lindheimer, M., Zaini, S., Keh, E., and Brun, B., Langmuir 2, 101 (1986).

57. Coughlan, B., Carrol, W.M., and McCann, W.A., J. Catal. 45, 332 (1976).

58. Barrer, R.M., and Cram, P.J., "Molecular Sieve Zeolites," (R. F. Gould, Ed.), Advan. Chem. Ser., 102, American Chemical Society, Washington, D. C., 1971, p.105

59. El-Alkad, T.M., Khalil, A.M., Attia, G., and Nashed, S.H., Surf. Technol. 14, 283 (1981).

60. Coughlan, B., Carrol, W.M., Kavanagh, P., and Nunan, J., J. Chem. Tech. Biotechnol. 31, 1 (1981).

61. Abo-El-Enein, S.A., Thermochim. Acta 31, 153 (1979).

62. Chessick, J.J., and Zettlemoyer, A.C., Adv. in Catalysis 11, 263 (1959).

63. Zettlemoyer, A.C., Ind. Eng. Chem. 57, 27 (1965).

64. Everett, D.H., and Wightman, J.P., Unpublished Results

65. Gregg, S.J., and Sing, K.S.W., "Absorption, Surface Area and Porosity", Academic Press, New York (1967).

66. Coughlan, B., and Carrol, W.M., J. Chem.Coc., Faraday Trans. I 72, 2016 (1976).

67. Coughlan, B., Carrol, W.M., and McCann, W.A., J. Chem. Soc., Faraday Trans. I 73, 1612 (1977).

68. Dekany, I., Szanto, F., Nagy, L.G., and Beyer, H.K., J. Colloid Interface Sci. 112, 261 (1986).

69. Messow, V. Quitzsch, K., and Herden, H., Zeolites 4, 255 (1984).

70. Rossin, J.A., PhD. Dissertation, VPI & SU, Blacksburg, VA (1986).

71. Dubinin, M. M., Advan. Colloid Interface Sci. 2, 2 (1965).

72. Shultz-Sibbel, G. M. W., Gjerde, D. T., Chriswell, C. D., Fritz, J. S., and Coleman, W. E., Talanta 29, 447 (1982).

73. Von Ballmoos, R., and Meier, W. M., Nature 389, 782 (1981).

74. Lyman, C. E., Betteridge, P. W., and Moran, E. F., "Intrazeolite Chemistry," (M. J. Comstock, Ed.), ACS Symposium Ser. 218, American Chemical Society, Washington, D. C., 1983, p.199

75. Kiselev, A. V., Disc. Faraday Soc. 40, 205 (1965).

76. Chen, N. Y., J. Phys. Chem. 80, 60 (1976).

The vita has been removed from the scanned document